Physica Medica 140 (2025) 105682

Contents lists available at ScienceDirect

Physica Medica

journal homepage: www.elsevier.com/locate/ejmp

Review paper

Comparative effectiveness of advanced radiotherapy techniques for brain cancers: A systematic review with an emphasis on dosimetric variability

Hamed Zamani [a], Mohsen Saeb [b], Shahram Monadi [b], Mostafa Alizade-Harakiyan [a,c], Ali Akhavan [d], Amin Khodaei [e], Mikaeil Molazadeh [a,f,*], Alireza Farajollahi [a,f,g,*]

[a] Department of Medical Physics, School of Medicine, Tabriz University of Medical Sciences, Tabriz, Iran
[b] Rasa Imaging and Therapy Center, Isfahan Healthcare City, Isfahan, Iran
[c] Radio-Oncology Department, Faculty of Medicine, Tabriz University of Medical Science, Tabriz, Iran
[d] Department of Radiotherapy and Oncology, School of Medicine, Isfahan University of Medical Sciences, Isfahan, Iran
[e] Faculty of Electrical and Computer Engineering, University of Tabriz, Tabriz, Iran
[f] Radio-oncology Department, Shahid Madani Hospital, Tabriz University of Medical Sciences, Tabriz, Iran
[g] Biotechnology Research Center, Tabriz University of Medical Sciences, Tabriz, Iran

ARTICLE INFO

Keywords:
Radiotherapy
High-grade glioma
Brain tumors
Treatment planning
Central nervous system

ABSTRACT

Background: Central nervous system (CNS) cancers pose a significant burden on global health. Radiotherapy remains central to treatment, yet optimal techniques for maximizing tumor control remain controversial due to dosimetric variability.

Methods: This systematic review evaluates the effectiveness of six advanced radiation techniques in clinical practice. Following PRISMA guidelines, we analyzed 61 studies from the Web of Science, PubMed, and Scopus, covering the period from 2018 to 2024, which reported on tumor coverage, dose conformity, and organ at risk (OAR) sparing.

Results: Our analysis revealed several key findings: (1) Tomotherapy (TOMO) demonstrated optimal dose homogeneity (HI 0.024-0.3) for hippocampal-sparing applications; (2) Volumetric Modulated Arc Therapy (VMAT) provided superior target coverage (CI 1.16-3.0) with greater efficiency (294 MU vs. Intensity-Modulated Radiation Therapy (IMRT 572 MU)); (3) Proton Beam Therapy (PBT) excelled in pediatric cases, reducing hippocampal dose by 91 % (4.8 Gy vs. 52.5 Gy); (4) Image-Guided Radiation Therapy (IGRT) enabled significant spinal cord sparing, with a Dmax reduction of 15 % compared to non-IGRT, through precise margin matching; (5) CyberKnife (CK) achieved remarkable accuracy for small lesions (<3 cm), maintaining the optic nerve dose below 2.02 Gy, although the treatment time averaged 220 min for larger targets. This review identified significant variability in OAR exposure across modalities (0.02 to 66.8 Gy), particularly for sensitive structures such as the brainstem (2.41 to 55.62 Gy).

Conclusions: While all modalities achieve acceptable tumor control, VMAT and PBT may provide advantages for complex geometries and pediatric cases, respectively. Prospective trials are needed to establish evidence-based guidelines for selection.

1. Introduction

Central nervous system (CNS) cancers encompass a range of diseases that are often resistant to treatment and classified as either primary tumors of the CNS or secondary metastases [1,2]. High-grade gliomas (HGGs) are particularly challenging to treat and have a poor prognosis [3]. Glioblastoma Multiforme (GBM) [4], a highly aggressive tumor affecting the CNS, is classified as the most severe form of astrocytoma subtype [2,5]. Despite various treatment options, these cancers frequently lead to significant mortality and morbidity across different age groups [1,6]. To achieve optimal clinical outcomes, various treatment strategies can be employed in multimodal therapy, including early surgical intervention, localized radiation therapy (RT), comprehensive craniospinal radiation, and chemotherapy. RT remains the cornerstone of treatment, but its effectiveness depends on maximizing tumor control while sparing vital structures (e.g., visual pathways, brainstem) [7].

* Corresponding authors at: Department of Medical Physics, School of Medicine, Tabriz University of Medical Sciences, Tabriz, Iran.
E-mail addresses: molazadeh91@gmail.com (M. Molazadeh), farajollahiar@gmail.com (A. Farajollahi).

https://doi.org/10.1016/j.ejmp.2025.105682
Received 19 April 2025; Received in revised form 6 October 2025; Accepted 28 November 2025
Available online 3 December 2025

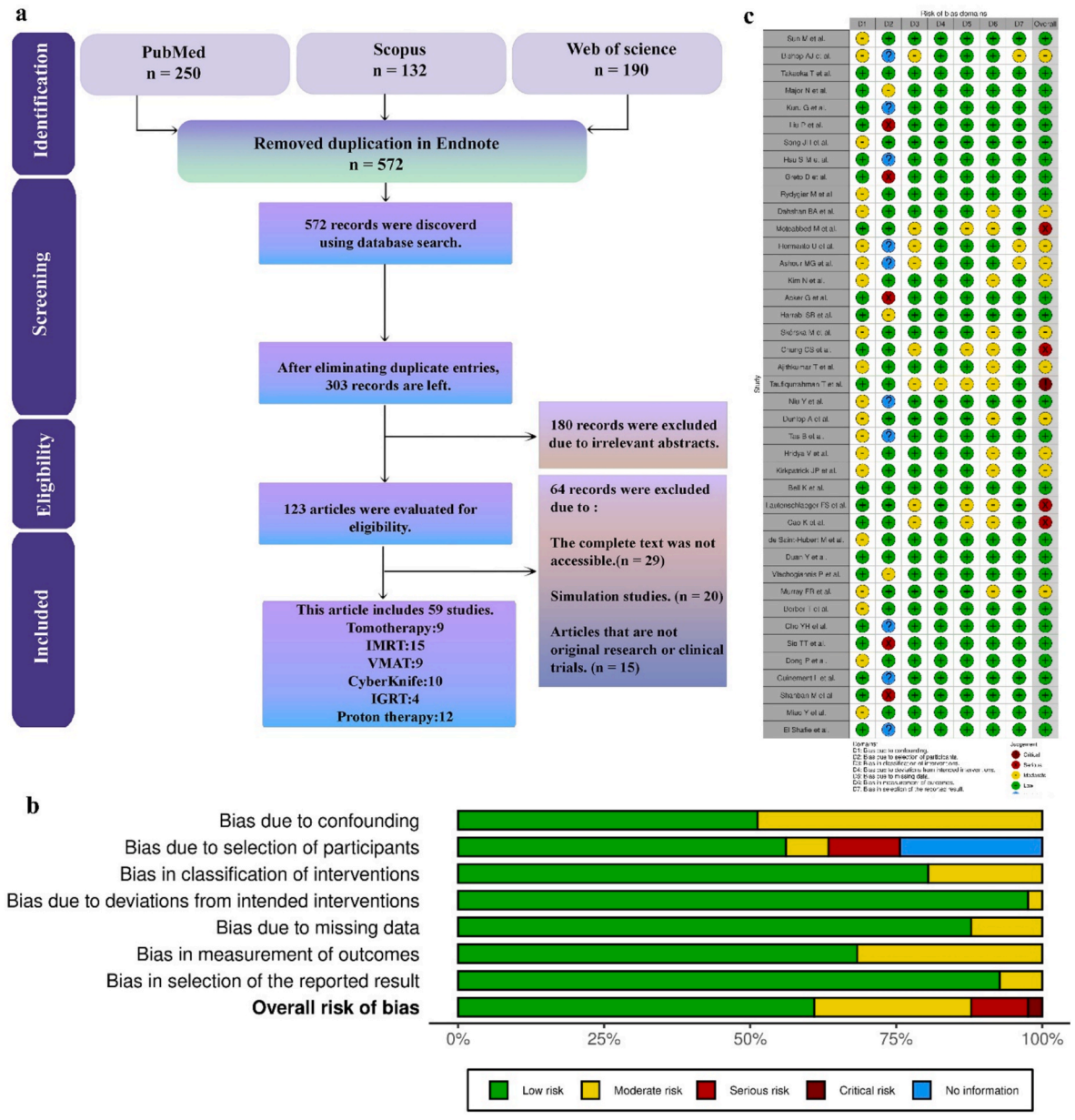

Fig. 1. Systematic Review Methodology and Assessment of Risk-of-Bias. a) Diagram illustrating the PRISMA flow chart for systematic reviews. b) Overall risk of bias and c)Risk-of-bias assessment (traffic light plot).

Over the past two decades, technological advancements have transformed RT from conventional 3D conformal (3DCRT) techniques [8] to exact modalities like the development of Tomotherapy (TOMO) [9], Intensity-modulated radiation therapy (IMRT) [10], Image-guided radiation therapy (IGRT), and Volumetric modulated arc therapy (VMAT). Further innovations—including proton beam therapy (PBT) with Bragg peak advantage and stereotactic radiosurgery (SRS) platforms such as CyberKnife (CK)—have expanded the treatment window for complex cases [11]. IMRT, in particular, is gaining recognition for its ability to control tumors while minimizing damage to healthy tissues effectively. However, the optimal RT approach for CNS tumors remains debated, with variability in reported outcomes across techniques. For instance, while PBT excels in pediatric OAR sparing, its cost and limited accessibility constrain widespread adoption. Similarly, IMRT and VMAT show dosimetric trade-offs in target coverage versus delivery efficiency [12,13]. Helical tomotherapy (TOMO), a variant of IMRT, provides advantages, such as small segments, multiple angles, and effective intensity modulation [14]. Helical TOMO treats the target area slice-by-slice [15], reducing radiation exposure to critical structures and reducing toxicity compared to traditional methods [16,17].

Recent advancements in radiotherapy, such as proton treatment, aim to mitigate harmful long-term effects while preserving healthy tissues. Adapting radiation regimens to various molecularly defined disease groups, whether as stand-alone treatments or in combination with novel targeted therapies, may pose significant challenges in the future. Additionally, high- and very-high-risk scenarios require innovative combinatorial treatments [18].

This systematic review evaluates six advanced RT modalities (TOMO, IMRT, IGRT, PBT, VMAT, and CK) in CNS cancers, focusing on dosimetric outcomes, clinical efficacy, and OAR reduction. Furthermore, it examines technique-specific adaptations for molecularly classified tumor subtypes and explores emerging combination strategies. We synthesize the available evidence to identify optimal approaches to minimize toxicity while maintaining tumor control. Our findings provide evidence-based clinical recommendations. Finally, we highlight critical knowledge gaps and future research directions to advance the

Table 1
Basic characteristics of brain tumor patients treated with the tomotherapy technique.

Treatment modality	Cancer type	Dose rate/ MU	Dose(Gy)/ Energy	Target Coverage		PTV	Main results (OAR)	Ref
				CI	HI			
TOMO	Glioma	3170 ± 0.97	D 98 % = 50.30 ± 0.13 D 50 % = 51.10 ± 0.15 D 2 % = 51.86 ± 0.15 /6 MV	1.21 ± 0.18	0.024 ± 0.002	198.6—310.4 cm^3	The OARs in the treatment include the optic chiasm with a Dmax of 27.64, the left eye, the right eye, the left lens with a Dmax of 3.03, the right lens with a Dmax of 2.76, the left optic nerve with a Dmax of 16.68, the right optic nerve with a Dmax of 16.79, the brain stem, the spinal cord, and both the left and right parotid glands with a Dmax of 14.85. Additionally, the use of TOMO was associated with a more favorable DHI compared to VMAT and IMRT.	[14]
	Whole brain	––	D 98 % = 26.7 ± 0.95 D 50 % = 32.8 ± 0.13 D 2 % = 33.8 ± 0.91/ 6MV	1.30 ± 0.09	1.50 ± 0.07	1486 cm^3	OARs include the hippocampus (D_{max} = 14.7), scalp (D_{max} = 31.7), optic nerves (D_{max} = 30.2), chiasm (Dmax = 31.8), right eye (D_{max} = 32), and left eye (D_{max} = 31.8). Dmax of the hippocampus was slightly higher in IMPT than in HT.	[21]
	brain metastases	––	30 Gy 6 MV	0.96	0.24	1200–1800 cc	The radiation doses delivered to various critical structures during treatment include 2 Gy to the brain stem, 14 Gy to the eye, 29 Gy to the optic nerve, 18 Gy to the hippocampus, and 43 Gy to the optic chiasm.	[22]
	Multiple Brain Metastases	15,576 600 MU/ min	18 Gy in the single fraction/ 6MV	1.34	1.08	10.5 cc	The Dmax and Dmean received by various structures are as follows: the right optic nerve (Dmax) received 0.91 Gy, while the left optic nerve received 1.3 Gy, and the optic chiasm received 0.95 Gy. The brain stem had a Dmax of 2.41 Gy. For the eyes, the right eye received a Dmax of 1.67 Gy and the left eye received 1.68 Gy. The right lens had a Dmax of 0.55 Gy, and the left lens had a Dmax of 0.72 Gy. Mean doses for the hippocampi were recorded at 0.64 Gy for the right hippocampus and 0.5 Gy for the left hippocampus. Both the right and left cochleae received a mean dose of 0.18 Gy, while the pituitary gland received a mean dose of 0.34 Gy. Lastly, the spinal cord had a Dmax of 0.1 Gy.	[23]
	High-Grade Glioma	––	60 Gy to PTV 1 and 50–54 Gy to PTV2/ 6 MV	PTV1: 0.98 ± 0.03 PTV2: 0.98 ± 0.05	PTV1: 0.09 ± 0.03 PTV2: 0.17 ± 0.05	PTV1:V95 (%) 98.52 ± 3.66 PTV2:V95 (%) 98.26 ± 5.27	The Dmax for various structures in high-grade glioma patients are as follows: the PRV for the brain stem had a Dmax of 55.62 ± 5.52 Gy; the left lens recorded a Dmax of 4.56 ± 1.73 Gy; the right lens had a Dmax of 4.44 ± 1.67 Gy; the left optic nerve received a Dmax of 38.46 ± 18.48 Gy; the right optic nerve had a Dmax of 32.67 ± 18.65 Gy; the optic chiasm recorded a Dmax of 47.06 ± 7.63 Gy; and the pituitary gland had a Dmax of 47.75 ± 17.03 Gy. In this context, HT demonstrates superior outcomes in terms of dose homogeneity, conformity, and sparing of OARs compared to IMRT and VMAT.	[24]
	Scalp	13 088	60 Gy/6MV	1.35	1.15	––	In the comparison between VMAT and HT, the following dose metrics were observed: for the brain, the ratio was 1.48; for the brain stem, it was 1.72; for the hippocampus, it was 1.39; for the left eyeball, it was 1.19; for the right eyeball, it was 1.31; for the left lens, the ratio was 2.00; for the right lens, it was 2.29; for the left optic nerve, the ratio came to 1.24; and for the right optic nerve, it was 1.83.	[25]
	Brain	––	A dose of 6 Gy/6 MV	0.47 0.68 0.84	1.20 1.17 1.23	403 cm^3	Among the three treatment modalities studied, the cone-based linac had the best conformity. The dose gradient of the FFF-VMAT linac for large tumors (28 mm in diameter) was better than that of TOMO, whereas TOMO had a better dose gradient than the FFF-VMAT linac for small tumors (8 mm in diameter). The dose gradient of the FFF-VMAT linac for large tumors (28 mm in diameter) was better than that of TOMO, whereas TOMO had a better dose gradient than the FFF-VMAT linac for small tumors (8 mm in diameter). TOMO or Cone base with couch at 0° for treatment.	[26]
	Single brain metastasis		12 to 22 Gy	1.20	1.06	6.32 cm^3	The capability of TOMO in delivering both homogeneous and heterogeneous dose distributions could be useful in the case of disease localized in	[27]

(*continued on next page*)

Table 1 (*continued*)

Treatment modality	Cancer type	Dose rate/ MU	Dose(Gy)/ Energy	Target Coverage		PTV	Main results (OAR)	Ref
				CI	HI			
							critical areas or in the case of retreatment, where a homogenous dose distribution could reduce the risk of radionecrosis.	
	Childhood Craniopharyngioma	––	50.4–54 Gy at 1.8 Gy per fraction	95 % CI: 3.46	––	3.6 cm^3	Evaluated the effects of PBT and IMRT on juvenile craniopharyngiomas in terms of toxicity, cyst dynamics, and disease control. It was discovered that PBT and IMRT generated comparable results in terms of survival and the control of solid and cystic illnesses.	[28]

Abbreviations: Conformity index (CI), Homogeneity index (HI), Normal tissue (NT), Clinical target volume (CTV), Maximum dose (Dmax), Gross tumor volume (GTV), Hippocampus avoidance (HA), Tomotherapy (TOMO), Intensity-modulated proton therapy (IMPT), Intensity-modulated radiation therapy (IMRT), Organs at risk (OAR), Stereotactic radiation therapy (SRT), dose heterogeneity index (DHI), planning risk volume (PRV), gross tumor volume (GTV), lifetime attributable risk (LAR), dose-volume histogram (DVH), relative biological effectiveness (RBE), plan quality index (pQI), and stereotactic radiosurgery (SRS).

field of CNS radiation oncology.

2. Methods

A literature review was conducted and reported according to PRISMA guidelines [19]. The PRISMA checklist is available as a supplementary document (S1 Document).

2.1. Inclusion and exclusion criteria

Articles were selected based on specific inclusion and exclusion criteria. To qualify for inclusion, published studies must meet the following criteria.

I. Clinical studies or experimental treatment planning studies must employ valid research designs with clearly defined methodologies and be written in English.
II. The study should specifically investigate the effects of radiation on brain cancers.

The following exclusion criteria were applied.

I. Systematic reviews, *meta*-analyses, conference proceedings, theses, and letters to the editor were excluded.
II. Studies involving computer simulations, including the Monte Carlo, Geant4, and Gate methods, were not included.
III. Articles focusing on other types of radiation, such as photo or ultrasound radiation, were excluded.

2.2. Quality assessment

Two investigators (HZ and MM) independently assessed the quality of the eligible studies before inclusion in the review using The ROBINS-I was used to assess methodological quality and risk of bias for non-randomized controlled trials. This tool includes an assessment of seven potential sources of bias, including confounding bias, participant selection bias, intervention classification bias, bias due to deviation from the intended interventions, bias due to missing data, bias in outcome measurement, and selection bias [20]. Notably, no studies were excluded based on the risk of bias assessment.

2.3. Search strategy, design, and study selection

Three databases, namely Web of Science, PubMed, and Scopus, were searched for this review. The search terms used in each database were: (((Brain cancers [Title/Abstract]) AND ((("Radiotherapy" [Mesh]) OR "IMRT" [Title/Abstract]) OR "IGRT" [Title/Abstract])) AND (((Glioblastoma multiforme [Title/Abstract]) OR "Glioma" [Mesh])). The search covered the period from March 2018 to December 2024. Additionally, a manual search of the reference lists of the review articles was conducted to identify potentially relevant studies. Two reviewers independently evaluated titles and abstracts. If an article met the inclusion criteria, its full text was reviewed. The same two reviewers assessed the eligibility of the selected articles through full-text evaluation. Any discrepancies were resolved through a discussion with a third reviewer. The study selection process was summarized using the PRISMA flow diagram (Fig. 1a).

2.4. Data extraction

Following the data extraction, the collected information was organized into tables using Microsoft Word. The results of the systematic literature search were compiled in EndNote 21 from various databases. After the final selection process, essential information was extracted and summarized in an extraction table. The data gathered from each study included several factors: treatment modality, cancer type, MU (monitor units), dose/energy, target coverage, PTV(planning target volume), and exposure time. This information was collected to assess its potential impact on the results.

3. Results

3.1. Study selection

The study flowchart in Fig. 1a outlines the search process. We identified 280 studies in PubMed, 151 in Scopus, and 201 in the Web of Science. After removing duplicates, we evaluated the titles of the 632 studies. Of the 403 records eligible for abstract review, 198 were excluded because their abstracts did not meet the inclusion criteria. Subsequently, we reviewed the full texts of 205 studies. Ultimately, we included 61 studies in this systematic review; the remaining studies did not satisfy the inclusion criteria. Details regarding the reasons for exclusion can be found in the Supporting Information (S1 Document).

3.2. Types of treatment

Our systematic review was organized and compiled into seven distinct tables. Tables 1–6 focus on and describe various treatment modalities related to advanced radiotherapy techniques, including TOMO, IMRT, IGRT, VMAT, CK, and PBT. Each table provides detailed insights into the specific characteristics and applications of these treatment methods, and the seventh table presents a comprehensive comparison of the different treatment options, facilitating a clearer understanding of their relative effectiveness and clinical relevance. This structured presentation aims to enhance comprehension and enable a thorough examination of various approaches to RT.

Table 2
Basic characteristics of brain tumor patients treated with IMRT technique.

Treatment modality	Cancer type	Dose rate (MU)	Dose/Energy	Target Coverage		PTV	Main results (OAR)	Ref
				CI	HI			
IMRT	Brainstem	––	Total doses ranged from 50 Gy to 61.20 Gy (the dose per fraction varied from 1.8 to 2 Gy).	cIMRT (1.27), ncIMRT (1.31)	0.078 (0.052–0.410) 0.137 (0.055–0.466)	The median PTV volume was 240.6 cc, with a range of 11.7 cc-687.1 cc	The OARs included the lenses, eyes, optic nerves, chiasm, and brain stem.HT and n-cIMRT were superior to cIMRT in terms of target conformity. Significantly, the n-cIMRT led to superior preservation of the eyes and lenses compared to HT.	[27]
	Brain		D 98 % = 25 D 50 % = 28.5 D 2 % = 29.3	––	0.40–0.42	––	Fractionated LINAC-based IMRT was superior concerning the HI in comparison to IORT and SRS methods.	[29]
	Brain		172.8 MeV and 51.3 Gy	––	––	79.2 cm^3, median 76.6 cm^3, minimum 17.0 cm^3, and maximum 170.3 cm^3 5 mm isotropic expansion	Two IMRT plans with different numbers of fields (5 and 7, except for patient 3 with fields 5 and 6) were used for each patient.	[30]
	Brain		D min = 44.0 ± 2.4 D max = 62.3 ± 0.9	2.24	––	Which ranged from 180 to 763 cm3 for initial PTVs, and 18 to 273 cm3 for boost PTVs	OAR structures, including the brainstem, optic chiasm, optic nerves, orbits, lenses, and the whole brain, were limited to a maximum dose of 54 Gy.	[31]
	Brain		D 98 % = 97.1 ± 0.7 D 50 % = 99.9 ± 0.3 D 2 % = 102.8 ± 0.6	––	0.58 ± 0.0114	PTV max = 105.9 ± 1.5 PTV min = 72.1 ± 11.5	The Average scalp dose can be reduced by around 45 % without compromising PTV coverage.	[21]
	Glioma		50.4 Gy with 1.8 Gy per fraction	––	––	195.2 cm^3	The total exposure of patients during pediatric brain cancer treatment has been estimated through the integration of various Monte Carlo-based dosimetry tools. This demonstrates that PBT significantly decreases out-of-field doses and the risk of secondary cancers in certain organs.	[29]
	Glioma	–-	60 Gy in 30 fractions D 98 % = 62.0 D 50 % = 34.3	0.88–1.80	––	511.7 cm^3	OARs are Brainstem (D_{max} = 54 Gy), Eyeball (D_{max} = 45 Gy), Optic apparatus (D_{max} = 54 Gy), Lens (D_{max} = 7 Gy), Cochlear (D_{max} = 35 Gy), and Spinal cord (D_{max} = 50 Gy). 21.0 % of patients developed severe radiation-induced lymphopenia, and it contributed to poor overall survival.	[32]
	Brain metastases	––	30 Gy/6 MV	0.96	0.25	1200–1800 cc	Brain Stem, Lens 5 Gy, eye 20 Gy, Optic nerve 35 Gy, Hippocampus 16 Gy, optic chiasm 45 Gy.	[22]
	Grade II gliomas	572	Dmean = 51.60 ± 0.27 Gy/6 MV	1.136 ± 0.009	0.032 ± 0.003	198.6—310.4 cm3	The Dmean to various structures is reported as follows: the right lens received a Dmean of 3.51 ± 0.16 Gy, while the left lens received a Dmean of 1.91 ± 0.20 Gy. The right optic nerve received a Dmean of 10.83 ± 2.77 Gy, and the left optic nerve received 11.34 ± 3.91 Gy. The optic chiasm had a Dmean of 17.05 ± 4.58 Gy, the pituitary gland (hypophysis) received 11.92 ± 4.26 Gy, and the brain stem had a mean dose of 16.92 ± 5.17 Gy. This data is essential for assessing the potential risks to these critical structures during radiation therapy.	[14]

(*continued on next page*)

Table 2 (*continued*)

Treatment modality	Cancer type	Dose rate (MU)	Dose/Energy	Target Coverage		PTV	Main results (OAR)	Ref
				CI	HI			
	High-Grade Glial Tumors	789 ± 112	60 Gy/30 Fr 2 Gy/6 MV	0.40–0.42	HI1: 0.17 HI2: 0.15 HI3: 0.17 HI4: 1.17	––	The Dmean for the ipsilateral optic nerve was 28.31 ± 16.61 Gy, while the Dmax was 37.69 ± 14.37 Gy. The optic chiasm received a Dmean of 28.03 ± 19.69 Gy, and the Dmax was 60.08 ± 0.92 Gy. Additionally, the brain absorbed 28.17 ± 20.47 Gy. For the eyes, the left eye received a Dmean of 28.61 ± 15.01 Gy, and the right eye received 37.69 ± 14.37 Gy. This information is crucial for evaluating the safety and efficacy of radiation therapy in protecting surrounding healthy tissues while effectively targeting the tumor.	[38]
	Hippocampus- and Scalp-Sparing Whole Brain	––	30 Gy in 10 fraction/6-MV	1.14 ± 0.02	1.28 ± 0.05	The median volume of the WB target was 1486 cm3 (range, 1158–1601 cm3). The median volume of the hippocampus, HA region, and the scalp was 3.95 cm3 (range, 2.50–4.37 cm3), 26.6 cm3 (range, 20.3–28.0 cm3), and 321 cm3 (range, 238–388 cm3), respectively	The Dmean and Dmax for various structures are as follows: the hippocampus received a Dmean of 7.0 Gy, and the scalp had a Dmean of 10.0 Gy. The optic nerves both received a Dmax of 32.8 Gy, while the optic chiasm also received a Dmax of 32.8 Gy. The right eye received a Dmean of 26.7 Gy, and the left eye received the same Dmax of 26.7 Gy. This data is important for assessing the potential impact of RT on these critical structures.	[21]
	Brain metastases	––	1.063 Gy	––	––	––	The average value of the dose received by the OAR Brainstem is 62.2 cGy OAR Optic Chiasm: 81.1 cGy The results of the comparison range show that organs at risk receive a lower dose with the VMAT radiation technique compared to the IMRT radiation technique, but this is not very significant from the statistical test results.	[34]
	High-Grade Glioma	––	60 Gy to PTV 1 and 50–54 Gy to PTV2/6 MV	PTV1: 0.97 ± 0.04 PTV2: 0:76 ± 0:10	PTV1: 0:10 ± 0:04 PTV2: 0:18 ± 0:04	PTV1:V95 (%) 98:37 ± 3:45 PTV2:V95 (%) 97:56 ± 3:26	The Dmax for various structures is as follows: the planning target volume for the PRV received a Dmax of 56.74 ± 3.57 Gy. The left lens received a Dmax of 6.48 ± 2.35 Gy, and the right lens received 6.21 ± 2.29 Gy. The left optic nerve had a Dmax of 37.91 ± 19.04 Gy, while the right optic nerve received 34.56 ± 18.57 Gy. The optic chiasm reached a Dmax of 45.62 ± 11.11 Gy, and the pituitary gland received a Dmax of 48.35 ± 16.35 Gy. This information is vital for understanding the potential risks associated with radiation therapy for these critical structures. For high-grade glioma patients in the situation described above, Helical TOMO has superior outcomes in terms of homogeneity, conformity, and	[24]

(*continued on next page*)

Table 2 (*continued*)

Treatment modality	Cancer type	Dose rate (MU)	Dose/Energy	Target Coverage		PTV	Main results (OAR)	Ref
				CI	HI			
	Head and Neck Cancer	––	65 Gy and 54 Gy	0.77	0.12	––	OAR sparing as compared with IMRT/VMAT. The reported radiation doses are as follows: the brainstem received a Dmean of 36.1 Gy, and the optic chiasm experienced a Dmax of 44.8 Gy. The left optic nerve had a Dmax of 37.4 Gy, while the right optic nerve received a Dmax of 37.8 Gy. The whole brain had a Dmean of 12.6 Gy. This data is essential for evaluating the effects of RT on these critical regions of the brain.	[35]

Abbreviations: Conformity index (CI), Homogeneity index (HI), Normal tissue (NT), Clinical target volume (CTV), Maximum dose (Dmax), Gross tumor volume (GTV), Hippocampus avoidance (HA), Tomotherapy (TOMO), Intensity-modulated proton therapy (IMPT), Intensity-modulated radiation therapy (IMRT), Organs at risk (OAR), Stereotactic radiation therapy (SRT), dose heterogeneity index (DHI), planning risk volume (PRV), gross tumor volume (GTV), lifetime attributable risk (LAR), dose-volume histogram(DVH), relative biological effectiveness (RBE), plan quality index (pQI), stereotactic radiosurgery (SRS), the non-coplanar technique (n-cIMRT), intraoperative radiotherapy (IORT).

3.2.1. *Tomotherapy*

Table 1 summarizes the main characteristics of studies that used TOMO for cancer treatment. The search identified ten studies: four focused on whole-brain metastases [21–23,26], two on HGGs [14,24], and two on childhood craniopharyngioma and scalp-sparing treatments [25,28]. Three studies reported widely varying MU values, with rates of 3170 ± 0.97 [14], 15,576 [23], and 13,088 [25] used for treatment. Seven studies used an energy of 6 MV [14,21–26]. Among these, six studies reported a dose range of 30–60 Gy [14,21,22,24,25,28], with one delivering 60 Gy to PTV1 and 50–54 Gy to PTV2 [24]. Additionally, two studies administered doses of 12–22 Gy [27], one reported a dose of 6 Gy [26], and another delivered 18 Gy in a single fraction [23].

In terms of target coverage, more than half of the articles (n = 6) reported a Conformity Index (CI) ranging from 1.2 to 1.35 [14,21,23,25–27], whereas three articles had a CI below 1 [22,24,26] and one study up to 3 [28]. Furthermore, four studies achieved a Homogeneity Index (HI) ranging from 1 to 1.2 [23,25–27], while two studies reported values between 0.1 and 0.3 [22,24], and another presented a value of 0.024 [14]. One study noted a PTV ranging from 198.6 to 310.4 cm^3 [14], reflecting differences in dose uniformity within the target volume. These variations underscore the necessity of optimizing treatment plans to achieve an ideal balance between target coverage, conformity, and homogeneity.

Another study indicated that the median volume of the whole-brain target was 1486 cm^3, with a range of 1158–1601 cm^3 [21]. Additionally, three studies reported a PTV of approximately 10 cm^3 [23,27,28], and one study on HGGs revealed that 95 % of PTV1 was approximately 98.52 cm^3 and PTV2 was about 98.26 cm^3 [24].

A comparative analysis of various studies showed significant discrepancies in the maximum dose (Dmax) delivered to the OARs. For the optic chiasm, Dmax ranged from 0.95 Gy to 47.06 Gy [14,21,23,24], indicating differences in treatment protocols and planning techniques. The Dmax for the left optic nerve varied from 1.3 Gy to 38.46 Gy [23,24], reflecting variations in dose constraints and priorities. The brainstem's Dmax ranged from 2.41 Gy to 55.62 Gy [23,24], highlighting the influence of different treatment modalities and planning strategies on dose distribution. These discrepancies highlight the need for individual planning to save on OARs.

3.2.2. *IMRT*

Table 2 summarizes the key characteristics of the 16 studies that used IMRT for cancer treatment. The search identified 16 studies: 8 focused on whole-brain metastases [21,22,27,29–31,33,34], one focused on low-grade tumors [14], four on HGGs [24,29,30,32], and one focused on hippocampal and scalp-sparing treatments [21], and one on head and neck cancers [35].

Two studies reported widely varying MU values, with rates of 572 [14], 789 ± 112 [30] used for treatment. Ten studies have reported radiation doses. Among these, six studies used an energy of 6 MV [14,21,22,24,30,33]. Among these, nine studies reported a dose range of 30–60 Gy [14,21,22,24,27,30–32,35], with one study delivering 60 Gy to PTV1 and 50–54 Gy to PTV2 [24]. Additionally, two studies administered doses under 30 Gy [29,33], whereas one study reported a dose of 1.06 Gy [34].

The studies exhibited a wide range of CI and HI values. In terms of target coverage, more than half of the articles (n = 4) reported a CI ranging from 1 to 1.31 [14,21,27,32], whereas four articles had a CI below 1 [22,24,33,35] and one study in over 2 [31]. Furthermore, 3 studies achieved a HI ranging from 1 to 1.2 [21,32,35], while six studies reported values between 0.1 and 0.5 [21,22,24,27,29,33], and another presented a value of 0.024 [14].

Five studies noted a PTV ranging from 100 to 500 cm^3 [14,27,29,31,32], reflecting differences in dose uniformity within the target volume. These variations underscore the necessity of optimizing treatment plans to achieve an ideal balance between target coverage, conformity, and homogeneity. Another study indicated that the median volume of the whole-brain target was 1486 cm^3, with a range of 1158–1601 cm^3 [21]. Additionally, three studies reported a PTV of approximately below 100 cm^3 [21,23,30], and one study on HGGs revealed that 95 % of PTV1 was approximately 98.52 cm^3 and PTV2 was about 98.26 cm^3 [24].

A comparative analysis of various studies showed significant discrepancies in the Dmax delivered to the OARs. For the optic chiasm, Dmax ranged from 0.95 Gy to 47.06 Gy [14,21,23,24], indicating differences in treatment protocols and planning techniques. The Dmax for the left optic nerve varied from 1.3 Gy to 38.46 Gy [23,24], reflecting variations in dose constraints and priorities. The brainstem's Dmax ranged from 2.41 Gy to 55.62 Gy [23,24], highlighting the influence of different treatment modalities and planning strategies on dose distribution. These discrepancies emphasize the importance of individualized treatment planning to optimize OAR sparing.

3.2.3. *IGRT*

The main characteristics of the four studies that utilized IGRT for cancer treatment are highlighted in Table 3. The search identified four studies: two focused on whole-brain metastases [36,38], and two

Table 3
Basic characteristics of brain tumor patients treated with IGRT technique.

Treatment modality	Cancer type	Dose rate (MU)	Dose/ Energy	1		1	1	1
				1	HI			
IGRT	Brain metastases	––	6 MV	1.18 1.54 1.08 1.04	1.28 1.29	0.5 – 1, 1–5, 5–10 cc	When the metastasis size is larger than 5 cc, the size of the metastasis and HI lose their importance for pQI. Based on the correlation between HI, GI, CI, and the size of metastasis, we have decided that pQI should be $\leq$ 7.0 between 0.1 cc and 0.5 cc metastasis volume, pQI should be $\leq$ 6 between 0.5 cc and 1 cc metastasis volume, pQI should be $\leq$ 5.0 between 1 cc and 5 cc metastasis volume, and pQI should be $\leq$ 4.0 between 5 cc and 10 cc metastasis	[36]
	Brain	––	66 Gy in 33 fractions /6 MV	1.186 ± 0.190	0.174 ± 0.02	––	The doses recorded for various structures are as follows: the spinal cord received a dose of 40.77 ± 2.10 Gy, while the left parotid gland had a dose of 32.01 ± 7.10 Gy, and the right parotid gland received 38.09 ± 11.30 Gy. The larynx recorded a dose of 42.12 ± 12.00 Gy. In terms of the eyes, the left eye received 2.35 ± 1.60 Gy, and the right eye received 2.20 ± 1.20 Gy. The left optic nerve had a D1% of 3.15 ± 2.50 Gy, and the right optic nerve recorded a D1% of 3.62 ± 3.40 Gy. The brainstem was exposed to a dose of 40.44 ± 8.82 Gy, while the mandible absorbed 62.94 ± 4.00 Gy. The left cochlea received 14.11 ± 15.90 Gy, and the right cochlea received 17.97 ± 26.30 Gy. Lastly, the volume of healthy tissue (V5) had a mean dose of 27.46 ± 8.30 Gy. This data is important for assessing the impact of RT on both targeted and surrounding tissues.	[37]
	Brain Metastases	––	15/18/24 Gy	1.8 for a 1-mm margin 1.6 for 3-mm Margin	––	12–16 cm^3	Low rates of local recurrence and radionecrosis were seen in both cohorts, indicating that SRS was well tolerated. However, a 1-mm GTV expansion is more suitable due to the increased risk of RN with a 3-mm margin.	[38]
	Brain	1 MU	50 Gy (2 Gy daily)/1 MV,6 MV	0.63 ± 0.14	0.19 ± 0.14	The PTV is contoured directly with a safety margin of 5–10 mm to the tumor area	This study compares the effects of dose smearing due to positioning errors and additional imaging doses by setup verification for a group of patients with head and neck cancer.OAR sparing was mostly reduced as a result of dose spreading brought on by placement problems for this collective. The inaccurate location significantly affected target coverage, particularly for individual patients. Even at the cost of more imaging dose and time, the value of a comprehensive IGRT is evident when considering the two impacts that have been studied.	[39]

Abbreviations: Conformity index (CI), Homogeneity index (HI), Normal tissue (NT), Clinical target volume (CTV), Maximum dose (Dmax), Gross tumor volume (GTV), Hippocampus avoidance (HA), Tomotherapy (TOMO), Intensity-modulated proton therapy (IMPT), Intensity-modulated radiation therapy (IMRT), Organs at risk (OAR), Stereotactic radiation therapy (SRT), dose heterogeneity index (DHI), planning risk volume (PRV), gross tumor volume (GTV), lifetime attributable risk (LAR), dose-volume histogram (DVH), relative biological effectiveness (RBE), plan quality index (pQI), stereotactic radiosurgery (SRS).

focused on brain cancers [37,39]. One study reported 1 MU per gantry position from ° 0–90° [39]. Based on the data from these articles, one study delivered a dose of 66 Gy in 33 fractions using 6 MV energy [37]. Based on the data from these articles, one study delivered a dose of 66 Gy in 33 fractions using 6 MV energy [12]. Another study administered doses of 15, 18, and 24 Gy using 6 MV energy [38]. Additionally, a dose of 50 Gy was delivered at 2 Gy daily using both 1 MV and 6 MV energies [39]. In terms of target coverage, reported values ranged from 1.18 to 1.54, with a mean value of 1.186 ± 0.190 [36,37]. For specific margins, the values were reported as 1.8 for a 1-mm margin and 0.6 for a 3-mm margin [38]. Some articles noted values as low as 0.63 ± 0.14, reflecting varying degrees of targeting precision [38]. Three studies reported HI values ranging from 0.174 [37] to 1.29 [36], with one study reporting a value of 0.19 [39], demonstrating variability in dose uniformity within the target area. The PTV encompassed tumor areas with specified volumes of 0.5–1, 1–5, and 5–10 cc, demonstrating variance [36], corresponding to dimensions ranging from 12 to 16 cm^3 [38]. To enhance treatment accuracy and effectiveness, a safety margin of 5–10 mm was applied around the tumor [38], ensuring that the PTV adequately accounted for potential variations in treatment delivery. Recorded doses for various structures included the spinal cord (40.77 ± 2.10 Gy), left parotid gland (32.01 ± 7.10 Gy), right parotid gland (38.09 ± 11.30 Gy), larynx (42.12 ± 12.00 Gy), left eye (2.35 ± 1.60 Gy), right eye (2.20 ± 1.20 Gy), left optic nerve (D1% = 3.15 ± 2.50 Gy), right optic nerve (D1% = 3.62 ± 3.40 Gy), brainstem (40.44 ± 8.82 Gy), mandible (62.94 ± 4.00 Gy), left cochlea (14.11 ± 15.90 Gy), right cochlea (17.97 ± 26.30 Gy), and healthy tissue volume (V5) with a mean dose of 27.46 ± 8.30 Gy. Low rates of local recurrence and radionecrosis were observed, indicating that Stereotactic Radiosurgery (SRS) was well tolerated. A 1-mm GTV expansion is recommended because of the increased risk of radionecrosis associated with a 3-mm margin. The study also highlights the impact of dose smearing due to positioning errors and additional imaging doses from setup verification for head and neck cancer patients, underscoring the value of comprehensive IGRT

Table 4
Basic characteristics of brain tumor patients treated with VMAT technique.

Treatment modality	Cancer type	Dose rate (MU)	Dose/Energy	Target Coverage		PTV	Main results (OAR)	Ref
				CI	HI			
VMAT	Glioma	294 ± 12	D 98 % = 49.21 ± 0.19 D 50 % = 50.79 ± 0.15 D 2 % = 52.09 ± 0.09 /6 MV	1.164 ± 0.014	0.041 ± 0.003	198.6—310.4 cm^3	OARs include the optic chiasm (D_{max} = 27.80), left eye, right eye, left lens (D_{max} = 3.28), right lens (D_{max} = 3.33), left optic nerve (Dmax = 14.51), right optic nerve (D_{max} = 15.56), brain stem, spinal cord, and left and right parotid gland (D_{max} = 19.11). VMAT, using variable dose rate, gantry rotation speed, and MLC shapes, can deliver good dose coverage and uniformity in the target area.	[14]
	Glioma	363 ± 45	59,78 ± 3,19/6 MV	––	––	––	The Dmean for various structures was as follows: left lens 6.45 ± 2.27 Gy, right lens 6.28 ± 2.38 Gy, right optic nerve 22.63 ± 17.98 Gy, left optic nerve 23.17 ± 15.45 Gy, optic chiasm 25.25 ± 20.24 Gy, PTV 95 % 59.78 ± 3.19 Gy, brain 26.74 ± 3.42 Gy, left eye 20.39 ± 12.17 Gy, and right eye 32.90 ± 16.84 Gy. This data is crucial for assessing the efficacy and safety of radiation therapy on targeted areas and adjacent healthy tissues.PTV coverage, conformity, and homogeneity index were comparable for VMAT and IMRT plans. VMAT plans showed statistically significant differences in PTV max (64.835 ± 0.504 Gy, p = 0.039), Brain max (64.378 ± 0.565 Gy, p = 0.025), and Eye L. max (20.39 ± 12.17 Gy, p = 0.046) compared to IMRT. Other differences in mean doses were not statistically significant.	[30]
	Brain Metastases	15576/ 600 MU/min	18 Gy in a single fraction	1.34	1.08	10.5 cc	The recorded radiation doses for various anatomical structures are as follows: The Dmax was 0.91 Gy for the right optic nerve, 1.3 Gy for the left optic nerve, 0.95 Gy for the optic chiasm, 2.41 Gy for the brainstem, 1.67 Gy for the right eye, 1.68 Gy for the left eye, 0.55 Gy for the right lens, and 0.72 Gy for the left lens. The Dmean included 0.64 Gy for the right hippocampus, 0.5 Gy for the left hippocampus, 0.18 Gy for both the right and left cochleae, 0.34 Gy for the pituitary gland, and 0.1 Gy for the spinal cord. This information is crucial for evaluating the potential impact of RT on these sensitive structures and for reducing their exposure.	[23]
	Brain	––	1.009 Gy	––	––	––	The average value of the dose received by the OAR Brainstem: 54.0 cGy OAR Optic Chiasm: 75.6 cGy The results of the comparison range show that organs at risk receive a lower dose with the VMAT radiation technique compared to the IMRT radiation technique, but this is not very significant from the statistical test results.	[34]
	Glioma	––	60 Gy to PTV 1 and 50–54 Gy to PTV2/6 MV	PTV1: 0.97 ± 0.04 PTV2: 0.80 ± 0.10	PTV1: 0.11 ± 0.03 PTV2: 0.20 ± 0.03	PTV1:V95 (%) 98.46 ± 3.28 PTV2:V95 (%) 97.81 ± 2.96	For high-grade glioma patients, the Dmax received by various structures is as follows: The brainstem PRV received 57.57 ± 3.43 Gy, the left lens 5.96 ± 2.18 Gy, the right lens 5.87 ± 2.50 Gy, the left optic nerve 38.84 ± 19.27 Gy, the right optic nerve 34.17 ± 19.29 Gy, the optic chiasm 41.03 ± 11.07 Gy, and the pituitary gland 49.48 ± 16.37 Gy. Studies have shown that Helical TOMO provides better results regarding dose homogeneity, conformity, and sparing of OAR compared to IMRT and VMAT.	[24]
	Brain metastases	500–1,400 MU/min	3/5/8/10/12 Gy/ 6Mv	1.6	––	median metastasis size < 0.1 cc	Compare SI-VMAT against the CyberKnife M6 system for the radiosurgical treatment of 5–10 BM. SI-VMAT offers enhanced treatment efficiency, as compared to CyberKnife, but requires a compromise regarding conformity and integral dose to the healthy brain.	[40]
	Brain metastases	––	3/6/12 Gy/ 6MV	0.62 ± 0.06	0.49 ± 0.06	0.92 to 2.24 cc	For single small brain metastases, Cone-VMAT may be used as an alternative to GK-free centers.	[41]
	Scalp	1791	60 Gy/6MV	1.49	1.17	––	In comparing VMAT and HT, the following dosimetric values were observed: Brain at 1.48, Brain stem at 1.72, Hippocampus at 1.39, Left eyeball at 1.19, Right Eyeball at 1.31, Left lens at 2.00, Right Lens at 2.29, Left optic nerve at 1.24, and Right optic nerve at 1.83. These values are critical for assessing the radiation	[25]

(*continued on next page*)

Table 4 (*continued*)

Treatment modality	Cancer type	Dose rate (MU)	Dose/Energy	Target Coverage		PTV	Main results (OAR)	Ref
				CI	HI			
							dose distribution in various brain structures during treatment planning.	
	Brain tumor	––	6 Gy/6 MV	0.48, 0.73, 0.92	1.25, 1.19, 1.23	8, 18, 28 mm	Among the three treatment modalities studied, the cone-based linac had the best conformity. The dose gradient of the FFF-VMAT linac for large tumors (28 mm in diameter) was better than that of TOMO, whereas tomotherapy had a better dose gradient than the FFF-VMAT linac for small tumors (8 mm in diameter). The dose gradient of the FFF-VMAT linac for large tumors (28 mm in diameter) was better than that of TOMO, whereas tomotherapy had a better dose gradient than the FFF-VMAT linac for small tumors (8 mm in diameter). TOMO or Cone base with couch at 0° for treatment.	[26]
	Brain tumors	––	25 Gy/6MV	1.21	––	9.57 cm3	For treating large or complex brain lesions via hypofractionated radiosurgery, GK better spares the normal brain and delivers a higher target dose compared with LINAC-based CK/VMAT deliveries.	[42]

Abbreviations: Conformity index (CI), Homogeneity index (HI), Normal tissue (NT), Clinical target volume (CTV), Maximum dose (Dmax), Gross tumor volume (GTV), Hippocampus avoidance (HA), Tomotherapy (TOMO), Intensity-modulated proton therapy (IMPT), Intensity-modulated radiation therapy (IMRT), Organs at risk (OAR), Stereotactic radiation therapy (SRT), dose heterogeneity index (DHI), planning risk volume (PRV), gross tumor volume (GTV), lifetime attributable risk (LAR), dose-volume histogram (DVH), relative biological effectiveness (RBE), plan quality index (pQI), stereotactic radiosurgery (SRS), Gamma knife (GK).

despite the increased imaging dose and time.

3.2.4. VMAT

Table 4 outlines the key characteristics of the ten studies that utilized VMAT for cancer treatment. The search identified six studies focusing on whole-brain metastases [23,26,34,40–42], three on HGGs [14,30,60], and one on scalp-sparing techniques [61]. Five studies reported a wide range of MU values, with rates of 294, 363 ± 45 [14,30], and 15,576 or 600 MU/min [23] used for treatment. Additionally, MU rates vary from 600 to 1400 MU/min [40], with one study documenting 1791 MU [61]. All 10 studies provided information on the radiation doses. Among these, eight employed 6 MV energy [14,24–26,30,40–42], with doses ranging from 25 to 60 Gy. One study administered 60 Gy to PTV1 and 50–54 Gy to PTV2 [60]. Furthermore, two studies delivered total doses between 3 and 12 Gy [40,41], whereas another study provided 18 Gy in a single fraction [23]. Two studies reported doses in the range of 1–10, specifically 6 and 1.009 Gy [62,63]. With regard to the CI and HI, the findings revealed a broad spectrum of values. Five studies reporting CI indicated values greater than 1, ranging from 1.16 to 3 [14,23,25,40,42]. In contrast, two studies reported CI values below 1, ranging from 0.49 to 1[45,64], reflecting varying degrees of targeting precision. Three studies documented HI values from 0.19 to 1.32 [23,25,26], with three studies reporting HI below 1 [14,24,41]. Among the seven studies that addressed PTV volume, one study found a median metastasis size of less than 0.1 cc [40]. Another study indicated a range of metastasis sizes from 0.92 to 2.24 cc [41]. Two studies reported PTV volumes of approximately 10 cm^3 [23,65], with a median volume of 79.2 cm^3. Additionally, one study showed a PTV volume ranging from 198 to 310 cm^3 [14], while another study reported PTV1 at 98.4 cm^3 and PTV2 at 97.81 cm^3 [60]. VMAT demonstrated effective dose coverage and uniformity within the target area, with mean dose (Dmean) values for various structures, including the left lens (6.45 ± 2.27 Gy) and right optic nerve (22.63 ± 17.98 Gy). The VMAT and IMRT plans exhibited comparable PTV coverage, conformity, and homogeneity indices. However, VMAT revealed statistically significant differences in the PTV max (64.835 ± 0.504 Gy, $p = 0.039$) and brain max (64.378 ± 0.565 Gy, $p = 0.025$). The recorded radiation doses for various anatomical structures included the Dmax values for the right optic nerve (0.91 Gy) and brainstem (2.41 Gy). While VMAT resulted in lower doses to OARs than IMRT, the differences were not statistically significant. For patients with HGGs, the planning risk volume (PRV) for the brainstem was 57.57 ± 3.43 Gy.

Hybrid techniques demonstrated superior dose homogeneity and conformity compared to IMRT and VMAT. Stereotactic Image-guided Volumetric Modulated Arc Therapy (SI-VMAT) offers improved treatment efficiency compared to CK, but at the expense of conformity and integral dose to healthy brain tissue. Cone-VMAT serves as an alternative to centers without Gamma Knife (GK) capabilities for treating single small brain metastases. The dosimetric values for VMAT and HT included the brain (1.48) and brainstem (1.72). The cone-based linear accelerator exhibited the best conformity among the three evaluated treatment modalities.

3.2.5. CyberKnife

Table 5 highlights the main characteristics of the ten studies that employed CK for cancer treatment. The search identified 10 studies: six on brain metastasis [23,40,43,48–50], and four focused on brain tumors [44,46,66,67]. Several studies have reported widely varying MU numbers at rates of 150 per fraction [64], 950 MU/min [44], and 15,576 [23] used for treatment. Additionally, MU rates range from 600 to 1,400 MU/min [40], with some studies reporting 1,000 MU/min [46]. The total treatment time varied, with one study reporting 220 min [68]. These variations highlight the differences in treatment protocols and planning techniques across different studies. Five studies utilized 6 MV energy [40,64,67–69]. One study reported a dose range of 21–60 Gy [67]. Five fractions were used to deliver 25 Gy [44], and 18 Gy was administered in a single fraction [23]. Other studies have reported doses of 12, 10, 8, 5, and 3 Gy using 6 MV energy [40]. One study reported a dose of 19 Gy, ranging from 12 to 21 Gy [68], while another study administered 24 Gy, ranging from 15 to 30 Gy, over 1–5 fractions [66]. Additionally, 6 MV of energy was used to deliver 18 Gy, ranging from 15 to 22 Gy [68]. One study reported a dose of 35 Gy [70], and another study administered 30 Gy in a median fraction of 10. Finally, 22 Gy was delivered in a median fraction of 1 for SRS using 6 MV of energy [69]. Regarding target coverage, one article reported a CI between 1 and 3 [69], more than half of the articles (n = 7) reported a CI between 1.2 and 1.4, and two articles had a CI below 1[64,66], indicating varying degrees of precision in targeting. Additionally, seven studies achieved an HI ranging from 1 to 1.8, and two studies reported values between 0.1 and 0.7[64,66]. One study reported a median PTV volume of 16.53 cc, ranging from 0.99 cc to 79.2 cc [44]. Another study indicated a median metastasis size of less than 0.1 cc [40]. Additionally, PTV volumes

Table 5
Basic characteristics of brain tumor patients treated with CK technique.

Treatment modality	Cancer type	Dose rate (MU)	Dose/Energy	Target Coverage		PTV	Main results (OAR)	Ref
				CI	HI			
CK	Brain metastases	150 per fraction	2/5/12/18/21/24/25/30/27/30 Gy/6MV	0.81	0.19	98 % of the PTV	In comparing the two treatment modalities, CK administered a higher median dose to the GTV than HyperArc for the following structures: brainstem, eye, optic nerve, and inner ear. This suggests that while CK may effectively target the tumor, careful consideration regarding the doses received by surrounding critical structures is needed.	[43]
	Brain	950 MU/min	25 Gy in five fractions	1.168 ± 0·08 (1.06–1.40)	1·32 ± 0·07 (1·15–1·44)	PTV ranged between 0·99 and 79·2 cc with an average of 16·53 cc	Doses of OARs in treatment plans for CK are 0·02–15 Gy for the brainstem and 0·01–13·6 Gy for the optic pathway. The treatment plans made for CK exhibit better results in terms of nCI (1·168 ± 0·08 versus 1·173 ± 0·077), SI (0·885 ± 0·05 versus 0·877 ± 0·05) and GI (3·64 ± 0·5 versus 4·45 ± 1·25), while HI values are better for TrueBeam and CK is a better modality for the delivery of SRS/SRT to intracranial tumors except for dose homogeneity where TrueBeam offered better results.	[44]
	Brain Metastases	15,576 600 MU/min	18 Gy in a single fraction	1.38	1.15	10.5 cc	The Dmax for the right optic nerve was 2.02 Gy, for the left optic nerve 1.21 Gy, for the chiasm 2.57 Gy, for the brain stem 5.23 Gy, for the right eye 0.26 Gy, for the left eye 0.37 Gy, for the right lens 0.14 Gy, and for the left lens 0.12 Gy. The mean for the right hippocampus was 1.84 Gy, for the left hippocampus 1.27 Gy, for the right cochlea 1.66 Gy, for the left cochlea 0.84 Gy, for the pituitary 0.94 Gy, and the maximum dose for the spinal cord was 0.81 Gy.	[23]
	Brain Metastases	500–1,400 MU/min	12, 10, 8, 5, and 3 Gy/6Mv	1.2	––	median metastasis size < 0.1 cc	Compare SI-VMAT against the CK M6 system for the radiosurgical treatment of 5–10 BM. SI-VMAT offers enhanced treatment efficiency compared to CK, but requires a compromise regarding conformity and integral dose to the healthy brain.	[40]
	Brain	––	19 Gy (range: 12–21)	0.498–1.074	0.732	1.05 cm3 (range: 0.01–19.80)	In single fraction CK-SRS, dose constraints for OARs included limiting the optic pathway to 8.0 Gy in 0.2 cm^3 (maximum point dose of 10.0 Gy in 0.035 cm^3) and the brainstem to 10.0 Gy (or 7.0 Gy) in 0.35 cm^3 (or 1.2 cm^3), with a max point dose of 14.0 Gy in 0.035 cm^3. The eyes were typically not irradiated. The biologically equivalent dose of 2 Gy per fraction was calculated using the linear-quadratic model, with an α/β ratio of 2 Gy for normal brain tissue and 10 Gy for tumor tissue. Dose ranges for the PTV were 50.0–54.3 Gy for a single fraction, 36.0–42.8 Gy for three fractions, and 31.3 Gy for five fractions.	[45]
	Brain	1000 MU/min	24 Gy (i.e., range, 15–30 Gy), administered over 1 to 5 fractions	1.30 (1.10–1.76)	1.19 (1.07—–1.27)	21.96 cc	CK achieved better CI and HI, while ZAP-X exhibited better GI and a smaller irradiated volume for the normal brain. The superiority of CK's plan conformity was more pronounced for target sizes less than 1 cc and greater than 10 cc	[46]
	Brain	––	21—60 Gy/6Mv	1.02 ± 0.01	1.31 ± 0.04	2 mm/2% criteria	Deep learning-based methods are a promising way to obtain clinical RT doses quickly, efficiently, and accurately. They transformed the CK case beam information into matrix coding and fed it into a neural network for training. The Dmax and their p-values are: Brainstem 0.054, Chiasm 0.278, Left Optic Nerve 0.492, Right Optic Nerve 0.275, Pituitary 0.496, Left Cochlea 0.250, and Right Cochlea 0.301. The ipsilateral optic nerve received 54.7 ± 59.5 Gy, the contralateral optic nerve 25.6 ± 44.7 Gy, the ipsilateral inner ear 38.1 ± 41.4 Gy, the contralateral inner ear 9.2 ± 19.7 Gy, the optic chiasm 109.2 ± 103.2 Gy, the ipsilateral thalamus 433.1 ± 270.5 Gy, the contralateral thalamus 260.5 ± 243.9 Gy, and the ipsilateral SVZ 731.9 ± 639.9 Gy. The right optic nerve received 2.02 Gy, the left optic nerve 1.21 Gy, the chiasm 2.57 Gy, the brain stem 5.23 Gy, the right eye 0.26 Gy, the left eye 0.37 Gy, the right lens 0.14 Gy, and the left lens 0.12 Gy. The right hippocampus received 1.84 Gy, the left hippocampus received 1.27 Gy, the right cochlea	[47]

(*continued on next page*)

Table 5 (*continued*)

Treatment modality	Cancer type	Dose rate (MU)	Dose/Energy	Target Coverage		PTV	Main results (OAR)	Ref
				CI	HI			
							received 1.66 Gy, the left cochlea received 0.84 Gy, the pituitary received 0.94 Gy, and the spinal cord received 0.81 Gy. The left lens received 6.45 ± 2.27 Gy, the right lens 6.28 ± 2.38 Gy, the right optic nerve 22.63 ± 17.98 Gy, left optic nerve 23.17 ± 15.45 Gy, optic chiasm 25.25 ± 20.24 Gy, PTV 95 % 59.78 ± 3.19 Gy, brain 26.74 ± 3.42 Gy, left eye 20.39 ± 12.17 Gy, and right eye 32.90 ± 16.84 Gy. VMAT plans showed significant differences in PTV max (64.835 ± 0.504 Gy, p = 0.039), Brain max (64.378 ± 0.565 Gy, p = 0.025), and Eye L. max (20.39 ± 12.17 Gy, p = 0.046) compared to IMRT. Other differences were not statistically significant.	
	Brain metastases	––	18 Gy (range, 15–22)/6 MV	1.55 (1.18–2.21) 1.57 (1.20–2.30)	1.18 ± 0.06	2.50 cm^3 (range, 0.044–19.9)	According to RTOG_CI criteria, CK produced more homogenous plans with considerably lower mean and maximum doses than GK when comparing Gamma Knife and CK in patients with brain metastases.	[48]
	Brain metastases	––	35 Gy	1.2 ± 0.1	1.2 ± 0.0	17.6 cc (IQR, 12.8–23.7 cc)	for evaluating the therapeutic consequences in treating brain metastases (BMs) and comparing the dosimetric characteristics of Gamma Knife (GK) with CK. While the normal tissue volume receiving 90–10 % of the prescribed dose was considerably larger in CK by 1.26 times, the mean dose reaching the tumor was significantly higher in GK by 1.25 times.Fractionated CK for big BMs appears to be as safe and successful as single-fraction GK for small BMs, despite the slightly lower dosimetric features of CK. This suggests that fractionation is a useful method for improving efficacy and reducing toxicity in stereotactic radiosurgery for BMs.	[49]
	Brain metastases	––	30 Gy in a median fraction of 10 22 Gy in a median fraction of 1 for SRS/6-MV	1.06–3.01	1.79	tumour volume (> 12 cc vs. ≤ 12 cc)	This study's goal was to clarify how re-irradiation for locally recurring brain metastases utilizing CK SRS affected clinical outcomes.SRS re-irradiation for locally recurring (LR) brain metastases has shown a favorable rate for both local control and overall survival, with acceptable toxicity. Additionally, the female gender reported higher overall survival.	[50]

Abbreviations: Conformity index (CI), Homogeneity index (HI), Normal tissue (NT), Clinical target volume (CTV), Maximum dose (Dmax), Gross tumor volume (GTV), Hippocampus avoidance (HA), Tomotherapy (TOMO), Intensity-modulated proton therapy (IMPT), Intensity-modulated radiation therapy (IMRT), Organs at risk (OAR), Stereotactic radiation therapy (SRT), dose heterogeneity index (DHI), planning risk volume (PRV), gross tumor volume (GTV), lifetime attributable risk (LAR),dose-volume histogram (DVH(DVH), relative biological effectiveness (RBE), plan quality index (pQI), stereotactic radiosurgery (SRS).

Table 6
Basic characteristics of brain tumor patients treated with PBT technique.

Treatment modality	Cancer type	Dose rate (MU)	Dose/Energy	Target Coverage		PTV	Main results (OAR)	Ref
				CI	HI			
PBT	Whole brain	––	D 98 % = 28.1 ± 0.34 D 50 % = 32.0 ± 0.60 D 2 % = 33.8 ± 0.91	1.14 ± 0.02,	1.28 ± 0.05	Range,1158–1601 cm^3	OARs include the hippocampus (D_{max} = 15.4), scalp (D_{max} = 30.8), optic nerves (D_{max} = 32.8), chiasm (Dmax = 32.8), right eye (D_{max} = 26.7), and left eye (D_{max} = 26.7). HA-WBRT using IMPT is a promising treatment to prevent cognitive decline and alopecia.	[21]
	Glioblastoma	––	39 Gy (13 fractions)	––	––	12.1 to 32.1 cm3	The level of adverse events is low and in line with data reported in the literature for photon re-RT or the few reports on particle beam re-RT. Of course, the CIRT and FSRT reirradiation concepts used different radiation doses (45 Gy RBE versus 39 Gy), so a simple dose-related effect cannot be disproved with the data at hand.	[51]
	Glioblastoma	––	50.4–60 Gy	––	5.84 ± 5.42	V95 % (in %): 96.36 ± 5.26	The Dmax for various structures are as follows: the ipsilateral optic nerve received 56.2 ± 39.0 Gy, the contralateral optic nerve 36.4 ± 36.7 Gy, the ipsilateral inner ear 44.5 ± 37.6 Gy, the contralateral inner ear 12.5 ± 22.8 Gy, the optic chiasm 66.8 ± 35.7 Gy, the ipsilateral thalamus 83.5 ± 26.6 Gy, the contralateral thalamus 69.3 ± 35.2 Gy, and the ipsilateral SVZ 86.3 ± 22.1 Gy. The dose distribution of PRT is significantly superior when compared to conventional radiotherapy, particularly concerning OAR, which are considered essential for neurologic function and neurocognition, or which play an important role in terms of quality of life. PRT might lead to reduced treatment-related side effects.	[21]
	Glioma	––	54.0 Gy 6-MV	0.22 ± 0.13	5.84 ± 5.42	185.2 ml	In this paper, the Dmax obtained for different structures is as follows: ipsilateral optic nerve 59.5 ± 54.7 Gy, contralateral optic nerve 44.7 ± 25.6 Gy, ipsilateral inner ear 41.4 ± 38.1 Gy, 27.9 ± Gy, 19.9 ± Gy, 19.9 ± Gy. Optic chiasm 103.2 ± 109.2 Gy, ipsilateral thalamus 270.5 ± 433.1 Gy, contralateral thalamus 243.9 ± 260.5 Gy, and ipsilateral SVZ 639.9 ± 731.9 Gy.	[52]
	Brain cancer	––	54 to 70 Gy	0.007	0.175	31.66—818.47 cm^3	The paper presents Dmax values and their corresponding p-values as follows: Brainstem 0.054, Chiasm 0.278, Left Optic Nerve 0.492, Right Optic Nerve 0.275, Pituitary 0.496, Left Cochlea 0.230, and Right Cochlea 0.230.	[53]
	Brain cancer	––	40 Gy and 45 Gy	Lower 95 % CI: 0.32 Upper 95 % CI: 0.85	––	––	In contrast to photon radiation, PBT enables the administration of higher radiation dosage to the tumor while reducing the damage to nearby vital structures. There was no discernible increase in risk when PBT was used. Of recurrent cancers in contrast to photon treatment.	[54]

(*continued on next page*)

Table 6 (*continued*)

Treatment modality	Cancer type	Dose rate (MU)	Dose/Energy	Target Coverage		PTV	Main results (OAR)	Ref
				CI	HI			
	Craniopharyngioma	––	dose of 54 CGE (Cobalt Gray Equivalent) in 30 fractions	Covered by 95 % isodose to PTV(was 0.99) range 0.93–1.00)	––	61.77 cm^3 (range 27.81–328.73)	The average dose to the left hippocampal region was between 4.8 and 46 Gy (mean 26 Gy), while the average dose to the right hippocampal region was between 13.8 and 52.5 Gy (mean 25.5 Gy). PBT is an acceptable and well-tolerated treatment for craniopharyngioma, according to the results.	[55]
	Craniopharyngioma	––	50.4–54 Gy at 1.8 Gy per fraction	95 % CI: 0.29	––	4.5 cm	evaluated the effects of PBT and IMRT on juvenile craniopharyngiomas in terms of toxicity, cyst dynamics, and disease control. It was discovered that PBT and IMRT generated comparable results in terms of survival and the control of solid and cystic illnesses.	[28]
	Paragangliomas	––	50.4 Gy RBE; range: 45.0–67.0 Gy/6 MV	––	––	The gross target volume was 26.5 cm^3	The purpose of this study was to evaluate the safety and effectiveness of PBT for head and neck paragangliomas, which are uncommon benign tumors that grow near important anatomical features like vascular tissues and cranial nerves.Doses to relevant organs at risk: Brainstem (Dmax): 26.6, Cochlea (Dmax): 45.2, Homolateral: 0.1, Contralateral: 0.1, Homolateral: 39, Contralateral: 0.2, Pituitary gland (Dmean) :10.2, Homolateral:27.2 Contralateral:0.1	[56]
	Meningiomas	–-	Hypofractionated fashion (3–8 fractions, usually 5 or 6 Gy) with a mean dose of 21.9 Gy (range, 14–46 Gy)	95 % CI CTV 1.02 (0.98–1.06)	0.19 ± 0.14	mean target volume 13 cm^3	This study's objective was to assess hypofractionated high-energy proton therapy efficacy and safety as a supplement or main treatment forMeningiomas of WHO grade I. According to the study, protons are a viable substitute for other, more widely used radiation treatments for meningiomas, with a high chance of controlling tumor growth over the long term. Since the mean target volume in our material (almost 13 cm^3) was larger than in many other similar series in the literature, proton beams are especially intriguing for patients with relatively large tumors due to their physical and dosimetric characteristics (no dose delivered downstream of the target and high conformality even to irregularly shaped targets).	[57]
	Meningiomas	––	(median dose of 62.0 Gy (RBE); range, 54–68	95 % CI 82.2–96 %	––	21.4 cm^3 (range, 0–546.5).	This study aimed to determine predictive factors for radiation-induced toxicity and tumor control and evaluate big and highly complicated meningioma clinical outcomes with PBSPT in a large, single-institution cohort. Tumor control rates are lower in patients treated at recurrence, those with non-benign histologies, and those undergoing inadequate resection. The timing of PBSPT and local tumor control were important predictors of overall survival.	[58]

(*continued on next page*)

Table 6 (*continued*)

Treatment modality	Cancer type	Dose rate (MU)	Dose/Energy	Target Coverage		PTV	Main results (OAR)	Ref
				CI	HI			
	Glioma	209	50.4 Gy 1.8 Gy per fraction/ 6-MV	0.22–0.81	––	195.2 cm^3	The out-of-field dose equivalent during PBT is in all cases lower than photon therapy techniques, and ranges from 120 mSv in the thyroid down to 0.6 mSv in the testes. PBT yields the smallest total lifetime attributable risk (LAR) (0.6 %), which is a factor of 5, 6, and 4 lower when compared to 3D-CRT, IMRT, and VMAT, Respectively	[59]

Abbreviations: Conformity index (CI), Homogeneity index (HI), Normal tissue (NT), Clinical target volume (CTV), Maximum dose (Dmax), Gross tumor volume (GTV), Hippocampus avoidance (HA), Tomotherapy (TOMO), Intensity-modulated proton therapy (IMPT), Intensity-modulated radiation therapy (IMRT), Organs at risk (OAR), Stereotactic radiation therapy (SRT), dose heterogeneity index (DHI), planning risk volume (PRV), gross tumor volume (GTV), lifetime attributable risk (LAR), dose-volume histogram (DVH), (DVH), relative biological effectiveness (RBE), plan quality index (pQI), stereotactic radiosurgery (SRS).

ranged from 0.01 cm^3 to 19.80 cm^3, with an average of 1.05 cm^3 [66]. One study reported a PTV volume of 21.96 cc [66], while another study indicated a volume of 2.50 cm^3, ranging from 0.044 cm^3 to 19.9 cm^3 [68]. The interquartile range (IQR) for PTV volumes was 12.8 cc to 23.7 cc, with a median volume of 17.6 cc. Tumor volumes were categorized as greater than 12 cc versus less than or equal to 12 cc [70].CK administered a higher median dose to the GTV than HyperArc in the brainstem, eye, optic nerve, and inner ear. Doses of OARs in CK treatment plans ranged from 0.02–15 Gy for the brainstem and 0.01–13.6 Gy for the optic pathway. The CK treatment plans exhibited better results in terms of nCI, SI, and GI, whereas HI values were better for TrueBeam. The Dmax for the right optic nerve was 2.02 Gy, in the left optic nerve 1.21 Gy, for the chiasm 2.57 Gy, and the brainstem 5.23 Gy. SI-VMAT offers enhanced treatment efficiency compared to CK, but requires a compromise regarding conformity and integral dose to the healthy brain. CK achieved better CI and HI, whereas ZAP-X exhibited a better GI and a smaller irradiated volume for the normal brain. Deep-learning-based methods are promising for obtaining clinical RT doses quickly, efficiently, and accurately.

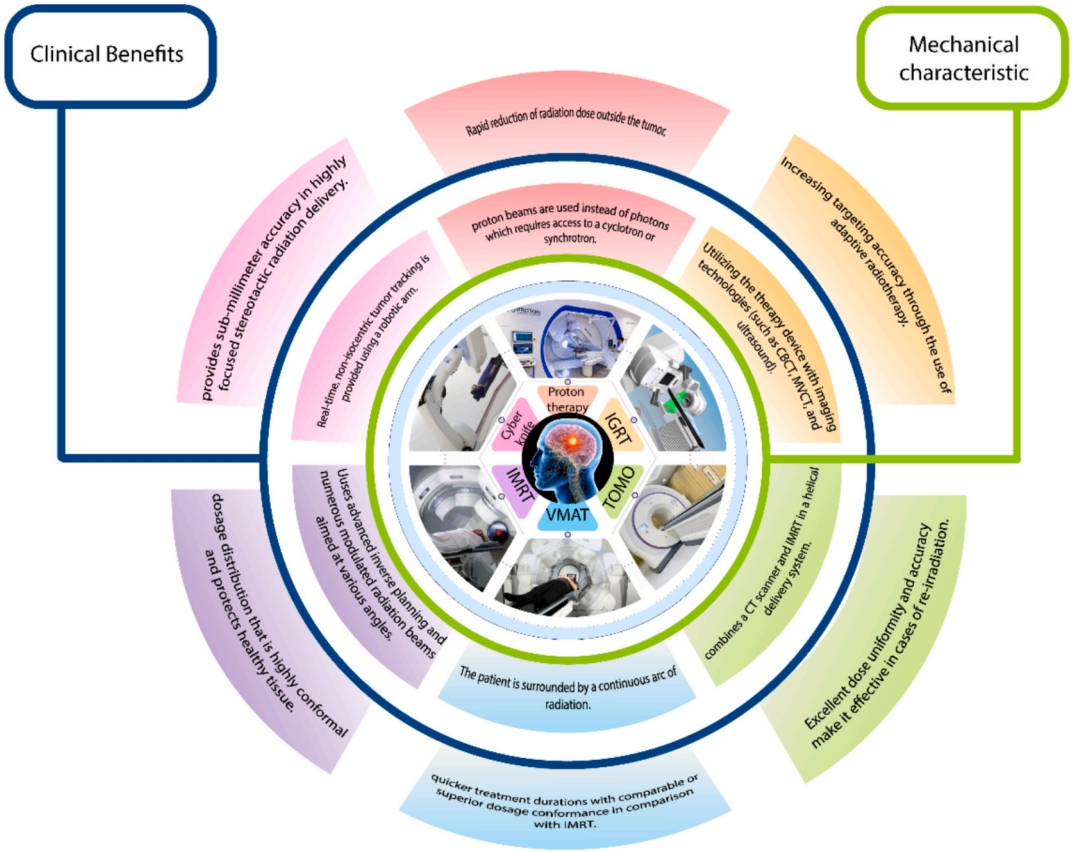

Scheme 1. Recent approaches in radiotherapy for brain cancers present six distinct modalities of radiation therapy, each offering significant advantages.

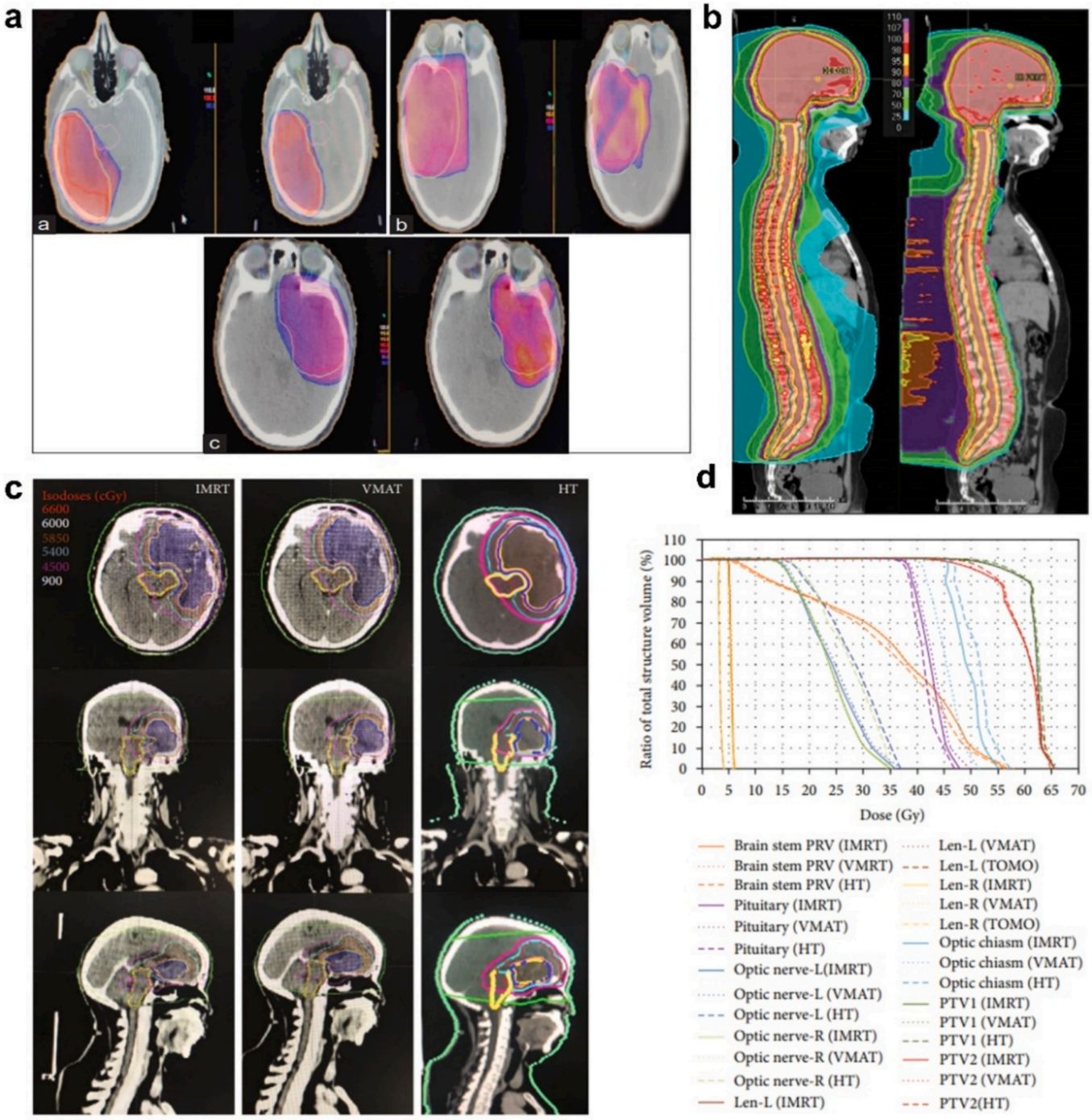

Fig. 2. Comparative Dose Distribution Analysis in Advanced RT Techniques for HGG Treatment: a) Axial slice images show the dose distributions obtained with IMRT (right) and three-dimensional conformal radiotherapy (left), with a 95 % isodose color wash for the PTV coverage for three different group scenarios. Reproduced from [65] under a Creative Commons CC BY-NC-SA 4.0). b) A comparison of the dose distribution between PBT and Helical TOMO for craniospinal irradiation. Reproduced from [65]under a Creative Commons CC BY-NC-SA 4.0). c) Single-patient dosage distributions for IMRT, VMAT, and Helical TOMO are shown. 66.00 Gy (red), 60.00 Gy (yellow), 58.50 Gy (orange), 54.00 Gy (cyan), 45.00 Gy (purple), and 9 Gy (green) are the doses indicated by the color-coded areas. Reproduced from [22] under a Creative Commons Attribution 4.0 International License (CC BY 4.0). d) A cohort of 42 individuals with HGG and the mean DVH for OARs is shown. Len-L for the left lens, Len-R for the right lens, Optic nerve-L for the left optic nerve, and Optic nerve-R for the right optic nerve. Reproduced from [22] under a Creative Commons Attribution 4.0 International License (CC BY 4.0). Abbreviations: Maximum dose (Dmax), Gross tumor volume (GTV), High-grade glioma (HGG), Tomotherapy (TOMO), Intensity-modulated proton therapy (IMPT), Intensity-modulated radiation therapy (IMRT), Organs at risk (OAR), Proton beam therapy (PBT), dose heterogeneity index (DHI), volumetric-modulated arc therapy (VMAT), dose-volume histogram (DVH).

3.2.6. PBT

Table 6 summarizes the key characteristics of the 11 studies employing particle beam radiation for cancer treatment. The search identified three studies focused on whole-brain metastasis [71–73], three on glioblastoma [73–75], two on craniopharyngioma [55,76], two on meningiomas [77,78], and one on paragangliomas [79]. Among the reviewed studies, three utilized 6 MV energy [59,75,79]. Seven studies reported dose ranges from 50.4 to 60 Gy, while one study delivered

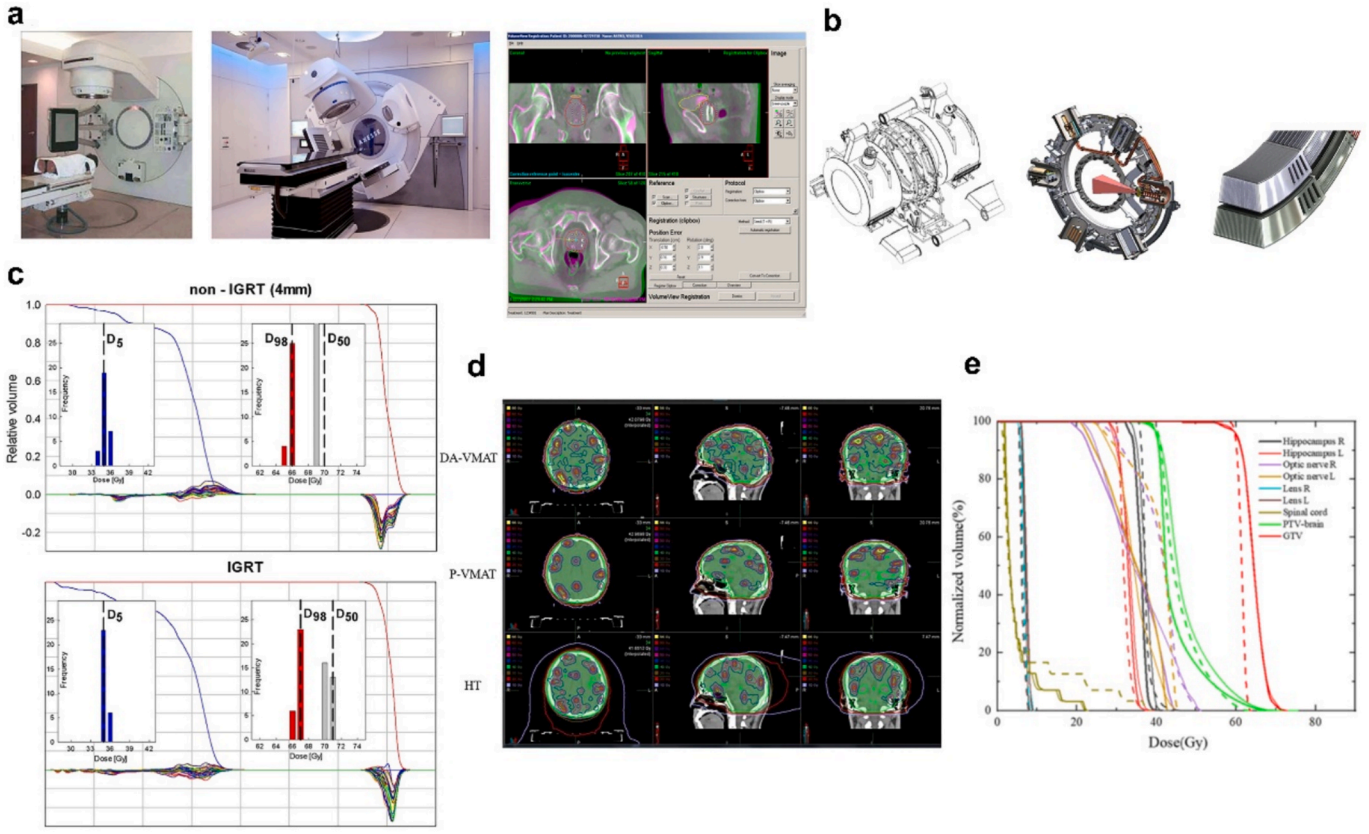

Fig. 3. Innovations in Radiotherapy Imaging and Dosimetry: A Comprehensive Overview of Advanced Systems and Treatment Planning: a) A modern integrated CBCT system and software platform for image reconstruction and analysis that exhibits a workflow-oriented architecture, as well as the initial CBCT prototype created by Jaffray and associates Reprinted from [91] under a Creative Commons Attribution 4.0 International License (CC BY 4.0).b) A 0.35 T split magnet MRI system with a revolving gantry that can hold a 6 MV linear accelerator is part of the ViewRay system. Additionally, a 138-leaf double-focused, double-stacked multileaf collimator is installed in this system. Reprinted from [91] under a Creative Commons Attribution 4.0 International License (CC BY 4.0). c)The DVHs for the CTV (red) and spinal cord (blue), as well as the corresponding fraction DVHs, are shown for both the IGRT and non-image-guided radiation therapy (non-IGRT) approaches. Additionally, to show the variation across all fractions, the D5 (blue), D98 (red), and D50 (grey) histograms are presented. Black dashed lines represent the planned values. Reprinted from [85] under a Creative Commons Attribution 4.0 International License (CC BY 4.0). d) A comparison of the dose distribution for HT, P-VMAT, and DA-VMAT (where red denotes GTV and green PTV-brain). Reprinted from [86] under a Creative Commons Attribution 4.0 International License (CC BY 4.0). e)A dose-volume histogram that shows the selected organs at risk in addition to the target volume. (Helical TOMO is shown by the dashed line, P-VMAT by the thick solid line, and DA-VMAT by the thin solid line). Reprinted from [86] under a Creative Commons Attribution 4.0 International License (CC BY 4.0). Abbreviations: Cone Beam Computed Tomography (CBCT), Gross tumor volume (GTV), High-grade glioma (HGG), Tomotherapy (TOMO), Intensity-modulated proton therapy (IMPT), Intensity-modulated radiation therapy (IMRT), Organs at risk (OAR), Proton beam therapy (PBT), dose heterogeneity index (DHI), volumetric-modulated arc therapy (VMAT), dose-volume histogram (DVH).

doses between 54 and 70 Gy. Additionally, two studies administered doses of 40 to 45 Gy, and one study used a dose of 39 Gy distributed over 13 fractions [72,74]. Another study reported a dose of 54 CGE (Cobalt Gray Equivalent), given in 30 fractions [55]. The Relative Biological Effectiveness (RBE) was found to range from 45.0 to 67.0 Gy, with a median RBE of 62.0 Gy [79]. Hypofractionated doses varied from 3 to 8 fractions, typically delivering 5 or 6 Gy per fraction, resulting in a mean dose of 21.9 Gy (range: 14 to 46 Gy) [77]. Regarding target coverage, three studies reported a CI between 1 and 1.2 [55,73,77], while others reported CI values below 1, indicating varying degrees of targeting precision. Additionally, two studies achieved HIs below 1 [71,77], two studies reported values between 5 and 6 [75,80], and one study presented a value of 1.28 [73]. One analysis indicated a PTV range from 1158 to 1601 cm^3, highlighting significant variability in target volume and underscoring the need for individualized treatment planning to ensure optimal dose distribution [73]. A smaller PTV range of 12.1 to 32.1 cm^3, along with a median V95% of 96.36 ± 5.26 %, indicates high dose coverage in smaller target volumes, which is crucial for effective treatment in localized cases [74,80]. Furthermore, an observed volume of 185.2 ml and a variability of 31.66 to 818.47 cm^3 illustrate the challenges of achieving uniformity in dose distribution across different PTV sizes [71,75]. Another finding detailed a PTV of approximately 61.77 cm^3, with an extensive range from 27.81 to 328.73 cm^3 [55], indicating that treatment responses can vary significantly based on target volume. Notably, for cases with a gross target volume of 26.5 cm^3 and a mean target volume of 13 cm^3, this variation emphasizes the critical role of precise targeting and dose optimization to maximize treatment efficacy [79]. Lastly, a PTV of 21.4 cm^3 (ranging from 0 to 546.5 cm^3) and a noted value of 195.2 cm^3 [59,78], highlight the complexity of balancing treatment objectives, necessitating continual refinement of planning strategies for optimal outcomes. These findings collectively underscore the importance of meticulous treatment planning and evaluation of PTV characteristics to ensure adequate target coverage while minimizing exposure to surrounding healthy tissue.

A comparative analysis across various studies reveals significant variations in the Dmax delivered to OARs. For the hippocampus, Dmax ranged from 4.8 Gy to 52.5 Gy, reflecting differences in treatment protocols and planning techniques. The Dmax for the scalp varied from 30.8 Gy, illustrating differences in dose constraints and treatment priorities. The Dmax for the optic nerves ranged from 1.3 Gy to 56.2 Gy, highlighting the impact of different treatment modalities and planning strategies on dose distribution. The Dmax for the optic chiasm ranged

Table 7
Comparison of complications (favorable or unfavorable) in the different radiotherapy modalities.

Type of RT	PBT	IMRT	VMAT	CK	IGRT	TOMO
Comparison of complications	IMPT achieved excellent hippocampus- and scalp-sparing. HA-WBRT using IMPT is a promising treatment to prevent cognitive decline and alopecia [53]. PRT is a highly conformal radiation technique offering superior dosimetric advantages over conventional radiotherapy by allowing significant dose reduction for organs at risk [21,98].	IMRT is not inferior to TOMO and VMAT and is still very suitable for treating most grade II glioma patients [14]. Both HT and n-cIMRT are capable of producing conformal and homogeneous treatment plans with good sparing of OARs. However, due to the non-coplanar capabilities of IMRT, n-cIMRT led to a superior dose reduction to the lenses [99].	The HyperArc technique seems to be more appropriate for multiple cranial metastases and large single metastatic lesions compared to the Cyberknife [43]. When the doses taken by the healthy brain tissue were evaluated in this study, the best protection was obtained from the IMAT plans [23].	The advantage of CK over SI-VMAT is the ability to provide better conformity and potentially lower integral dose to the healthy brain. While SI-VMAT enhances treatment efficiency for cases with multiple brain metastases, it does so at the expense of these dosimetric parameters. Additionally, CK's dedicated system may allow for more precise targeting without the larger PTV margins needed for treatments delivered by conventional linear accelerators, which can help minimize exposure to surrounding healthy tissue [40].	Where daily IGRT is routine clinical practice, 40–80 % reductions in margin sizes are possible. Widespread use of IGRT has given clinicians confidence to reduce CTV-PTV margins to 3 mm, reporting reduced patient toxicities with no reduction in local control [100].	The finest IMRT system to date is Helical TOMO, which combines IGRT and IMRT. It uses spiral CT rotation to take pictures and treat tumors, and it can provide dose-guided radiation or adaptive RT [14]. Daniela Greto et al. conducted a dosimetric evaluation of CK and TOMO treatment regimens for single brain metastases. In conclusion, TOMO and CK are excellent RS tools, and clinical guidance is required when deciding which to employ [27].

Abbreviations: Radiotherapy (RT), Tomotherapy (TOMO), Intensity-modulated proton therapy (IMPT), Intensity-modulated radiation therapy (IMRT), Organs at risk (OAR), Stereotactic radiation therapy (SRT), dose heterogeneity index (DHI), planning risk volume (PRV), gross tumor volume (GTV), lifetime attributable risk (LAR), dose-volume histogram (DVH), non-coplanar technique (n-cIMRT).

from 0.95 Gy to 66.8 Gy, demonstrating variability in treatment approaches. The brainstem's Dmax ranged from 2.41 Gy to 55.62 Gy, emphasizing the importance of individualized treatment planning to optimize OAR sparing while achieving therapeutic goals. These discrepancies reinforce the necessity for tailored treatment planning to balance OAR protection with effective cancer treatment.

3.3. Studies' risk of bias

Fig. 1b depicts a summary of the RoB-1 assessment. The evaluation of bias risk across the radiotherapy studies revealed a predominantly low-risk profile, with approximately 75 % of the studies being classified as low-risk. This indicates a robust methodological approach in the majority of the research conducted in this area. In contrast, around 15 % of the studies were assessed to have a moderate risk of bias, suggesting some concerns that could affect the validity of their conclusions. Furthermore, about 10 % of the studies exhibited serious bias in various domains, highlighting specific areas for improvement in future research. A closer examination of participant selection and missing data revealed that less than 5 % of the studies demonstrated serious bias in these critical areas. This finding underscores the meticulous attention to detail and rigorous methodology applied to participant inclusion and data management, indicating a strong commitment to research integrity. When assessing bias due to confounding variables, approximately 80 % of the studies were rated as having low risk. This is significant, as it suggests that the researchers effectively controlled for potential confounders that could skew the outcomes. Additionally, there were over 80 % of studies that were similarly rated low risk regarding deviations from planned interventions, further reinforcing the reliability of the findings. The classification of interventions within these studies appeared to be predominantly favorable, with around 90 % receiving a low-risk designation. In terms of outcome measurement, reliability also appeared strong, with around 85 % of the studies classified as low risk, indicating that the methods used to assess outcomes were robust and credible. Importantly, no studies in this review exhibited a critical risk of bias, which enhances the overall confidence in the findings. Only a small number of studies had insufficient information, indicating that transparency and completeness in reporting were largely upheld. these findings reflect a favorable bias profile and demonstrate strong reliability in the conclusions drawn regarding the effectiveness and safety of radiotherapy, suggesting that the evidence base for this treatment modality is both solid and trustworthy. Fig. 1c represents the traffic light plot of the risk of bias assessment for each included study.

Key findings showed significant variability in dose delivery: VMAT achieved a CI of 1.16–3.0, while CK demonstrated accurate OAR sparing (e.g., mean optic nerve dose: 2.02 Gy). PBT consistently reduced doses to critical structures (e.g., hippocampus Dmax: 4.8–52.5 Gy), particularly in pediatric cases. However, heterogeneity in study designs, target volumes, and reporting criteria limits direct comparisons between modalities. Notably, all techniques have clinical acceptance for tumor control, with VMAT and PBT showing potential benefits in complex geometries or sensitive anatomical regions. These results emphasize the need for standardized reporting and personalized planning. Below, we explore these findings in clinical practice and highlight gaps for future research.

4. Discussion

4.1. Key dosimetric comparisons across modalities

Modern radiotherapy techniques allow for steep dose gradients between OARs and target volumes, facilitating simultaneous differential dosing for whole-brain and metastatic lesions (Scheme 1). Simultaneous integrated boost (SIB) optimizes dose distribution and reduces treatment time and costs compared with sequential boosts, although sparing the hippocampus increases dose heterogeneity in normal brain tissue [63]. For oropharyngeal cancer, IMRT demonstrates lower toxicity than 2D/3D RT without compromising oncological outcomes and uses a seven-field inverse planning approach with 6 MV photons (Fig. 2(a)) [81–83]. Comparative studies highlight trade-offs between methods: VMAT achieves efficient target coverage (CI 1.16–3.0), while PBT reduces hippocampal Dmax by 30–50 % in children, which is critical for neurocognitive preservation. However, heterogeneity in study designs prevents definitive rankings and emphasizes the need for standardized protocols (Fig. 2(b)) [60,84].

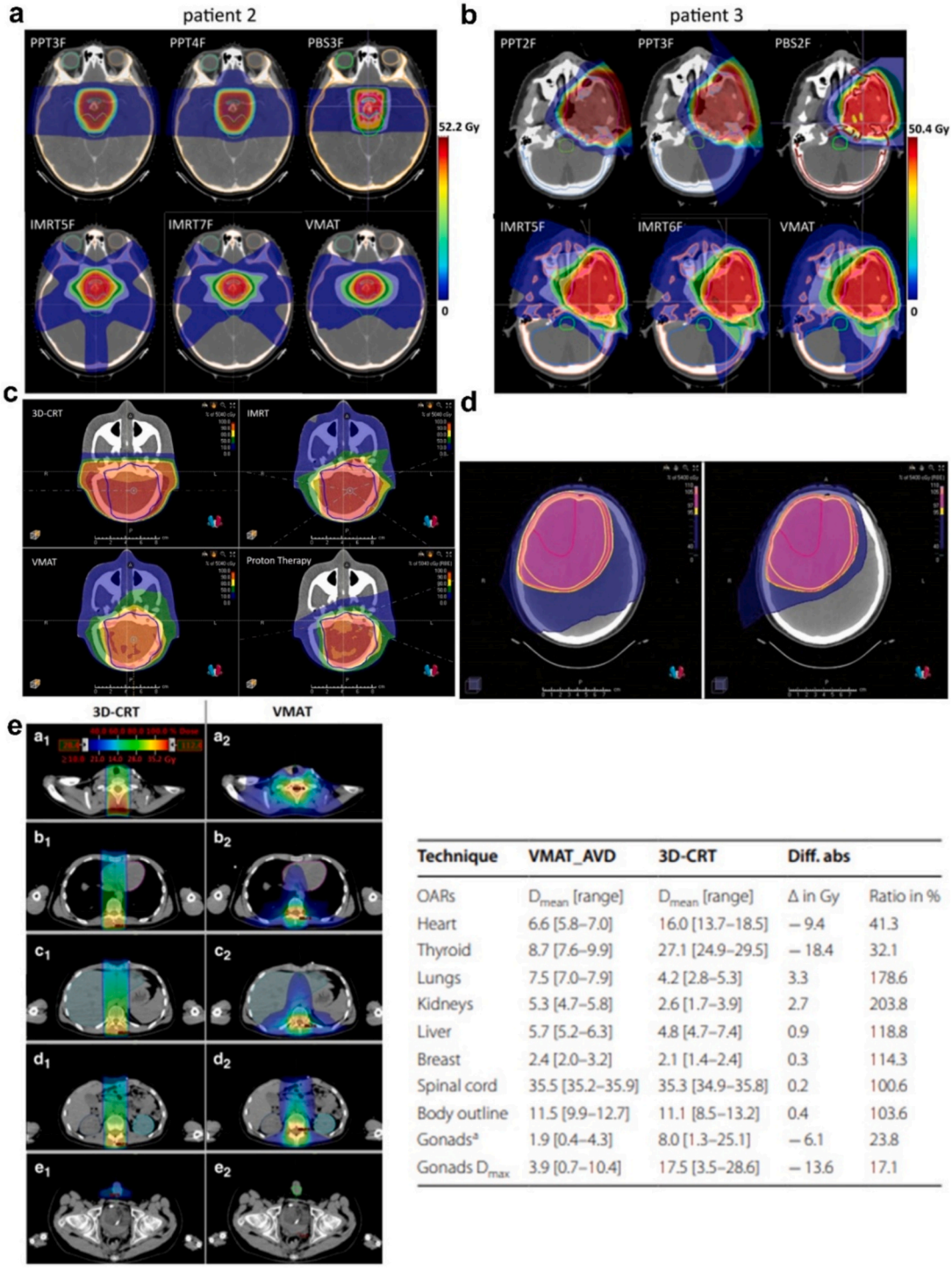

Technique	VMAT_AVD	3D-CRT	Diff. abs	
OARs	D_{mean} [range]	D_{mean} [range]	Δ in Gy	Ratio in %
Heart	6.6 [5.8–7.0]	16.0 [13.7–18.5]	−9.4	41.3
Thyroid	8.7 [7.6–9.9]	27.1 [24.9–29.5]	−18.4	32.1
Lungs	7.5 [7.0–7.9]	4.2 [2.8–5.3]	3.3	178.6
Kidneys	5.3 [4.7–5.8]	2.6 [1.7–3.9]	2.7	203.8
Liver	5.7 [5.2–6.3]	4.8 [4.7–7.4]	0.9	118.8
Breast	2.4 [2.0–3.2]	2.1 [1.4–2.4]	0.3	114.3
Spinal cord	35.5 [35.2–35.9]	35.3 [34.9–35.8]	0.2	100.6
Body outline	11.5 [9.9–12.7]	11.1 [8.5–13.2]	0.4	103.6
Gonads[a]	1.9 [0.4–4.3]	8.0 [1.3–25.1]	−6.1	23.8
Gonads D_{max}	3.9 [0.7–10.4]	17.5 [3.5–28.6]	−13.6	17.1

Fig. 4. Evaluation of Dosage Distributions Across Multiple RT Modalities: a)A comparison of the dosage distribution (transverse view) for patients 2 and 3 used a variety of modalities, such as PPT (3/2-field and 4/3-field), PBS (2-field and 3-field), IMRT (5-field and 7/6-field), and VMAT Reprinted with permission from [30] copyright 2014, Institute of Physics and Engineering in Medicine. b)Plans for 3D-CRT, IMRT, VMAT, and PBS proton therapy produced by the treatment planning system, showing isodoses and the PTV in blue. Reproduced from [97]under a Creative Commons CC BY-NC-SA 4.0). c) A comparison of the dosage distribution for proton beam therapy and helical tomotherapy in low-grade gliomas. Reproduced from [97] under a Creative Commons CC BY-NC-SA 4.0). d)Dose distributions for the spine PTV using the VMAT technique (right) and 3D-CRT approach (left), with a minimum dose threshold of 10 Gy (28.4 %). Reproduced from [102]under a Creative Commons CC BY-NC-SA 4.0). e)3D-CRT stands for three-dimensional conformal radiotherapy, whereas VMAT_AVD is a combination of volumetric modulated arc therapy and avoidance sectors. Reproduced from [102]under a Creative Commons CC BY-NC-SA 4.0). Abbreviations: Piggyback Proton Therapy (PPT), Pencil Beam Scanning (PBS), Intensity-modulated radiation therapy (IMRT), Organs at Risk (OAR), Proton beam therapy (PBT), dose heterogeneity index (DHI), volumetric-modulated arc therapy (VMAT), Image-guided Radiation Therapy (IGRT).

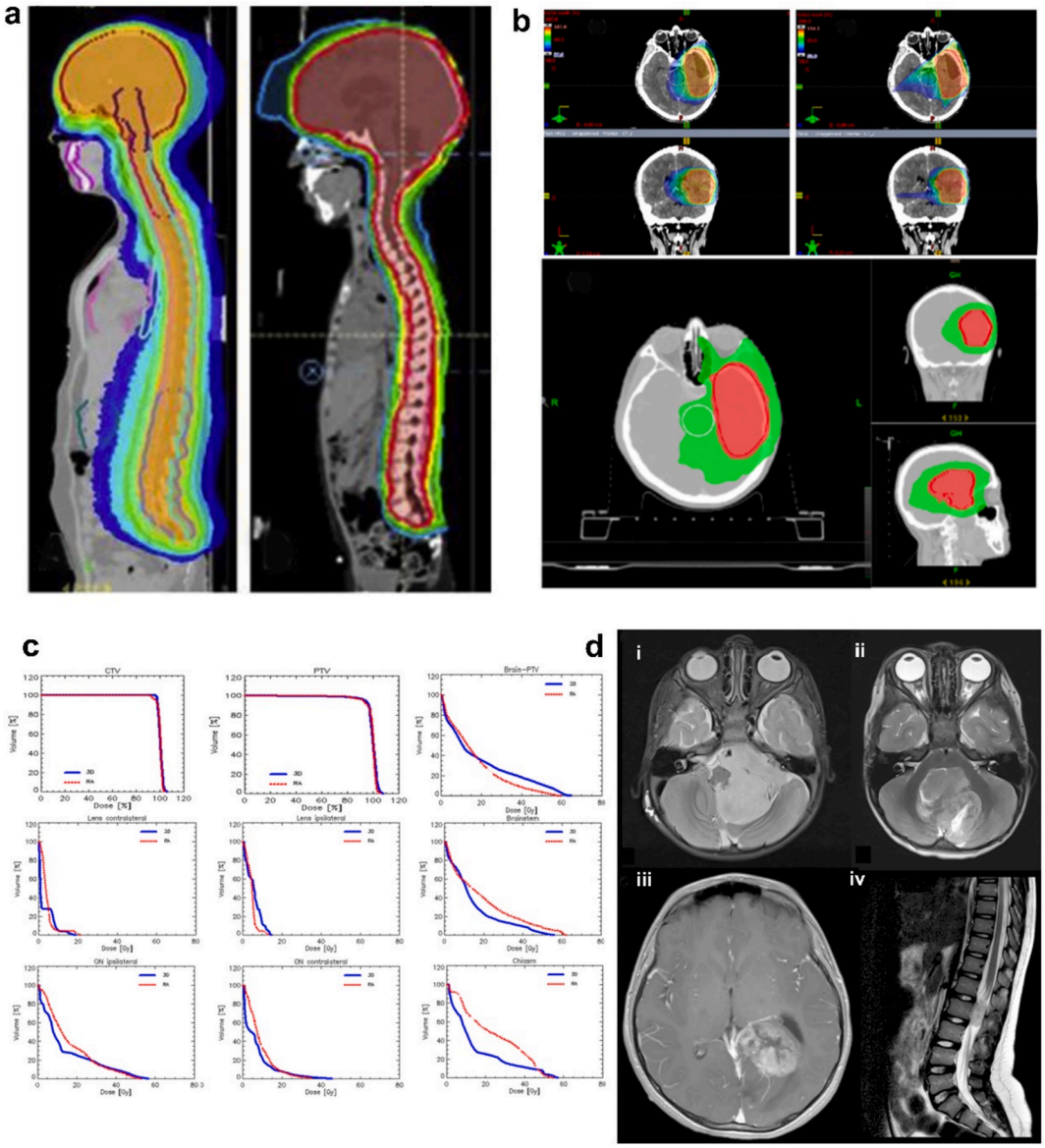

Fig. 5. Comparative Analysis of Dose Distributions and Imaging Techniques in Brain Tumor Treatment: a)Dose distribution in craniospinal irradiation using the left-photon and right-proton beam techniques. Reprinted with permission from [103] Copyright 2018, Elsevier B.V. b)The dose distributions in a typical example of grade II gliomas using TOMO, IMRT, and VMAT on the top left and right, respectively. Reproduced from [14] under the Creative Commons Attribution-NonCommercial-NoDerivs License (CC BY-NC-ND). c) DVH for both 3DCRT and VMAT approaches for CTV, PTV, and OARs. Reproduced from [104] under a Creative Commons Attribution 4.0 International License (CC BY 4.0). d) Pediatric ependymoma imaging illustrations. i) A large left cerebellopontine angle ependymoma that encloses the basilar trunk and lower cranial nerves causes the brainstem to rotate and shift, as shown in an axial T2-weighted sequence. ii) The fourth ventricle is destroyed by a midline posterior fossa anaplastic ependymoma (PFEPN-A), as shown by axial T2-weighted sequences. iii) A heterogeneously increasing supratentorial anaplastic ependymoma is depicted by an axial T1-weighted post-gadolinium sequence (STEPN-RELA). iv) An intradural extramedullary myxopapillary ependymoma at the L2 level that compresses the cauda equina is visible on a mid-sagittal T2-weighted sequence. Reprinted with permission from [105] Copyright © 2019, Springer Science Business Media, LLC, part of Springer Nature. Abbreviations: Clinical tumor volume (CTV), Planning tumor volume (PTV), High-grade glioma (HGG), Intensity-modulated radiation therapy (IMRT), Organs at risk (OAR), Proton beam therapy (PBT), Volumetric-modulated arc therapy (VMAT), dose-volume histogram (DVH).

Dosimetric analyses show subtle advantages. For HGGs, Liu et al. (2020) directly compared IMRT, VMAT, and TOMO, demonstrating that hybrid TOMO achieved superior target dose conformity (CI 1.05 ± 0.03 vs. 1.12 ± 0.04 for VMAT) and homogeneity (HI 1.08 ± 0.02 vs. 1.15 ± 0.03 for IMRT) while better sparing OARs (Figs. 2c,d). This supports TOMO's role for complex HGGs requiring integrated boost fields [60], while CK shows better preservation of normal tissue (brainstem, optic structures) compared to TrueBeam, with better gradient indices (GI 3.64 ± 0.5 vs. 4.45 ± 1.25) [44]. For multiple metastases, piecewise VMAT (P-VMAT) offers higher matching and lower V44 in normal brain tissue than HT or dynamic arcuate VMAT (DA-VMAT) [78]. IGRT reduces spinal cord Dmax by 15 % compared to non-IGRT, although both achieve comparable CTV coverage (Fig. 2(c, d)) [85].

4.2. *Clinical advantages in specific patient populations*

The pediatric population uniquely benefits from PBT. Craniopharyngioma treatment utilizes minimal PBT output dose to preserve endocrine and cognitive function [86]. For medulloblastoma, PBT reduces the risk of secondary cancer by sparing normal tissues during craniospinal irradiation (CSI), with a lateral dose distribution that favors VMAT_AVD over 3DCRT [18,87,88]. A 5-year phantom study confirmed a lower risk of secondary cancer in PBT with PBS compared with IMRT or 3DCRT [59]. In ependymoma (EPM), 3-year progression-free survival

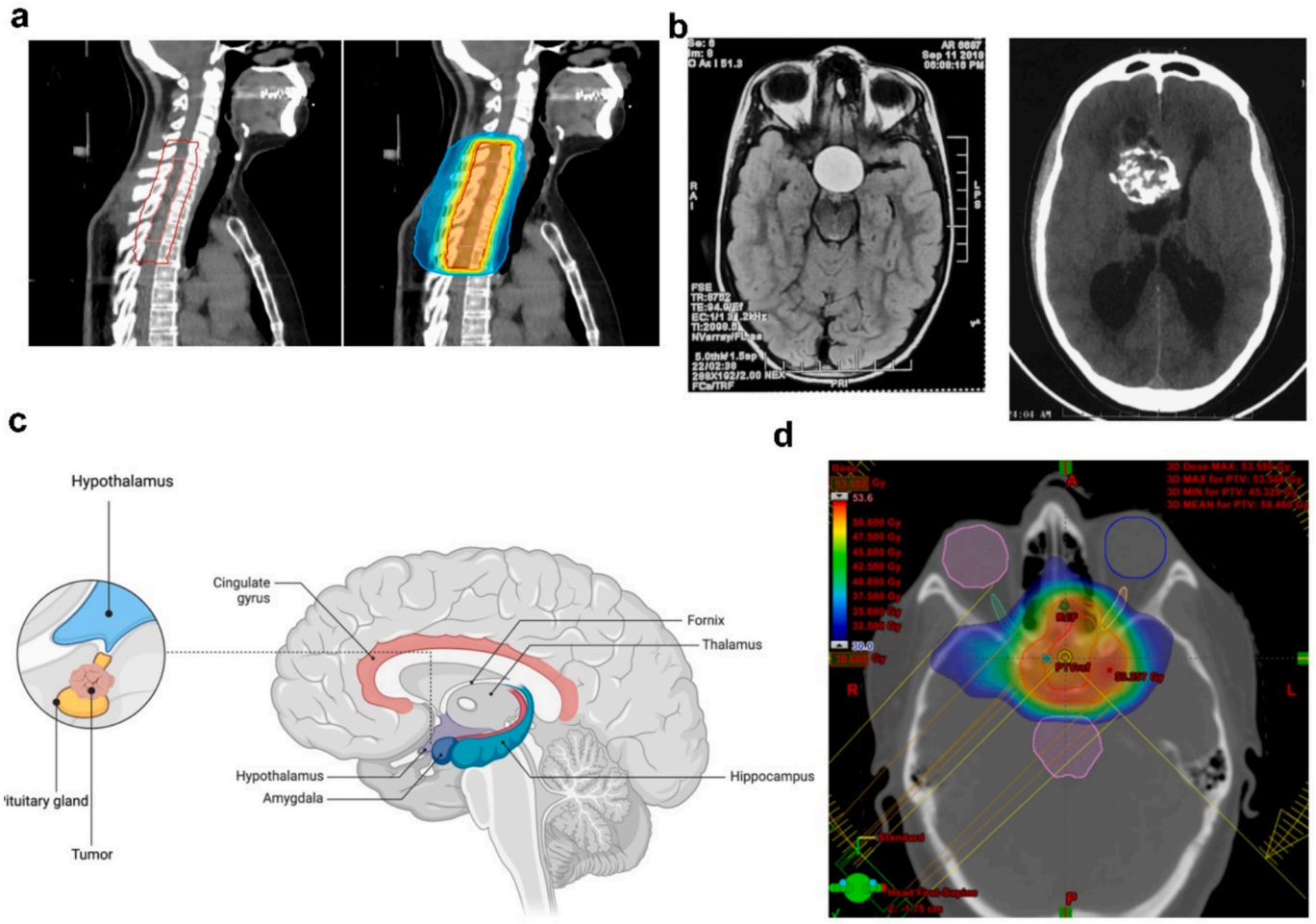

Fig. 6. Radiological and Treatment Insights for CNS Tumors. a) Postoperative radiation after subtotal resection is the treatment plan for a patient with spinal ependymoma, which is categorized as CNS WHO grade II. Reprinted with permission from [108]Copyright © 2024, Oxford University Press. b) A well-defined cystic lesion that occupies space in the sellar region is visible on FLAIR imaging in the axial plane. A non-contrast CT image showing a calcified cystic development in the suprasellar area linked to hydrocephalus is shown in the figure. Reprinted with permission from [109] Copyright 2024, International Institute of Anticancer Research. c) Craniopharyngiomas usually develop along the glandular tissue of the pars tuberalis that envelops the pituitary stalk, close to the pituitary glands and hypothalamus. Reproduced from [110]under a Creative Commons Attribution 4.0 International License (CC BY 4.0). d) A dosage distribution illustration for craniopharyngioma using 3D conformal treatment. Reprinted with permission from [111]Copyright © 2012, Springer Science Business Media, LLC. Abbreviations: Central nervous system (CNS), Computed tomography (CT).

with PBT is consistent with photon therapy while reducing side effects [89], although a small cohort study (N = 10 PBT vs. N = 22 photon) reported poorer survival with PBT, which warrants further investigation (Fig. 3(a-c))[90].

For adult gliomas, VMAT reduces moderate to high brain doses (V20Gy, V35Gy) compared to 3DCRT, albeit at a lower dose (V3Gy, V5Gy) [92]. Sun et al. (2023) quantified modality-specific trade-offs for grade II gliomas in a postoperative cohort: TOMO delivered significantly higher PTV-D98% (50.30 ± 0.13 Gy) versus VMAT (49.21 ± 0.19 Gy, *p*=0.006) and IMRT (49.78 ± 0.18 Gy, *p*=0.014), critical for marginal target coverage. However, IMRT retained advantages in lens sparing (Dmax 4.2 Gy vs. 7.5 Gy for TOMO) and brainstem protection (V45 < 0.5 cc vs. 1.2 cc for VMAT), while VMAT required fewer monitor units (294 ± 19 vs. 572 ± 24 for IMRT) (Fig. 3(d, e)) [14]. Management of craniopharyngioma benefits from the precision of IMRT and the efficacy of CK for residual/recurrent lesions, with no reported reduction in pituitary function after treatment [84,93].

4.3. Implementation challenges and limitations

Despite its dosimetric advantages, PBT faces access barriers: 80 % of low- and middle-income countries lack infrastructure and insurance coverage, which delays treatment by 6–8 weeks, which is critical for aggressive tumors such as GBM [18,94]. No RCTs have demonstrated a survival advantage of PBT over photons in adult gliomas, and VMAT achieves comparable control at one-third the cost [44,95]. The exceptional accuracy of CK (nCI 1.168 ± 0.08) is offset by impractical session times (220 min for a volume of 21.96 cc) [44]. IGRT spinal cord preservation requires an additional 20–30 min per session, which questions its utility in rapidly progressing HGG [96].

Modern radiotherapy techniques each offer distinct advantages for central nervous system tumors, with optimal selection depending on the clinical context. VMAT shows superior efficacy and comparable target coverage (CI 0.88–1.35) to IMRT, while reducing treatment time by 30–50 % (294 vs 572 MU). However, IMRT retains its advantage for highly precise cases and achieves a lower optic nerve Dmax (11.34 Gy vs 22.63 Gy for VMAT). PBT shows particular promise in pediatric cases, reducing hippocampal Dmax per photon to 4.8 Gy vs 52.5 Gy, although its high cost (100 K-200 K/cycle) limits access. For small lesions (less than 3 cm), CK provides excellent agreement (nCI 1.168 ± 0.08) but becomes impractical for larger targets due to the long session time (220 min for a volume of 21.96 cc) [92].

Table 8
A complete set of recommendations for clinical practice based on our tables and data analysis for selecting the optimal RT regimen.

Tumor Type	Clinical Scenario	Preferred Treatment Modality	Advantages	Limitations	Ref
GBM	Adult, unresectable	VMAT	– Balance of PTV coverage (CI = 1.16–3.0) and OAR reduction (optic nerve Dmax ~ 22 Gy)- Faster delivery (294 MU compared to 572 MU for IMRT)	– Less hippocampal reduction than PBT	[14,24,30]
	Pediatric or near-critical structures (e.g., brainstem)	PBT	– Superior OAR sparing (hippocampus Dmax 4.8 Gy vs. 52.5 Gy with photons)- Less neurocognitive toxicity	– Cost-prohibitive (100 K–100 *K*–200 K/course)- Limited availability	[21]
Grade II Gliomas	Postoperative	IMRT	– Better lens/brainstem protection (lens Dmax 1.9–3.5 Gy) – Lower MU (572 compared to 317 for TOMO)	– Longer delivery time than VMAT	[14]
Brain Metastases	Single lesion (<3 cm)	CK	– Best conformity (nCI = 1.168 ± 0.08)- Precise OAR sparing (optic nerve Dmax 1.2–2.0 Gy)	– Prolonged sessions (220 min for > 10 cc)	[23,43,44]
	Multiple lesions (≥3) or large (>3 cm)	VMAT	– Efficient treatment (15 min/session)- Acceptable conformity 1.16–1.6	– Higher integral brain dose than CK	[40,41]
	Whole-brain and hippocampal sparing	TOMO	– Homogeneous dose (HI = 0.024–0.19)- Scalp preservation (Dmax 31.7 Gy)	– Higher lens doses (3.0–4.5 Gy) vs. IMRT	[21,25]
Pediatric Tumors	Medulloblastoma/ Craniopharyngioma	PBT	– Minimizes cochlear/endocrine doses (cochlea Dmax = 0.1–12.5 Gy)- Reduces secondary cancer risk (LAR = 0.6 % vs. 3 % for photons)	– Requires anesthesia in young children	[28,55,59]
Ependymoma	Spinal or intracranial	IMRT	– Standard for spinal EPM- Comparable LC to protons in retrospective data	– PBT may offer superior sparing but lacks survival RCTs	[89,92]
Meningioma	Skull-base or large (>5 cm)	PBT	– Superior conformality for irregular shapes- Hypofractionation feasible (21.9 Gy/5 fx)	– Limited long-term toxicity data	[57,58]
Recurrent Tumors	Prior RT exposure	CK	– Precision retreatment (optic chiasm Dmax 2.6 Gy)- Adaptable to prior dose	– Risk of radionecrosis in central lesions	[45,50]

Abbreviation: Glioblastoma (GBM), Volumetric Modulated Arc Therapy (VMAT), Intensity-Modulated Radiation Therapy (IMRT), Proton Beam Therapy (PBT), CyberKnife (CK), TomoTherapy (TOMO), Planning Target Volume (PTV), Organ at Risk (OAR), Conformity Index (CI), Maximum Dose (Dmax), Monitor Units (MU), Homogeneity Index (HI), New Conformity Index (nCI), Local Control (LC), Lifetime Attributable Risk (LAR), Fractions (fx), Randomized Controlled Trials (RCTs), Gray (Gy).

Heterogeneous reporting and inconsistent variables across studies complicate comparisons between different methods. For example, while PBT reduces the maximum hippocampal dose to 4.8 Gy (versus 52.5 Gy with photons), its high cost ($100,000–200,000 per session) limits adoption [30,97]. Similarly, the dosimetric superiority of TOMO for HGGs is offset by its resource intensity (Table 7)[24].

4.4. Technical considerations for different tumor types

The choice of radiotherapy modality should be tailored to the specific tumor type and based on anatomical and clinical constraints. For gliomas, the standard paradigm involves maximal safe tumor resection followed by adjuvant radiotherapy, with a dose range of 45–60 Gy, delivered via adaptive techniques such as IMRT or VMAT. In LGGs, TOMO shows better target coverage with significantly higher PTV-D98% values (50.30 ± 0.13) compared with VMAT (49.21 ± 0.19) and IMRT (49.78 ± 0.18), although IMRT retains its advantages in sparing the lens and brainstem [14]. HGGs pose unique challenges due to their aggressive nature and proximity to critical structures such as the temporal lobe and brainstem. Here, VMAT shows dosimetric advantages over 3DCRT, particularly in reducing exposure to moderate-high doses (V20Gy and V35Gy) to healthy brain tissue, while 3DCRT performs better in low-dose areas (V3Gy and V5Gy) [92]. For brain metastases, technical considerations vary based on the size and multiplicity of the lesion.

The fractional VMAT approach offers an optimal balance of whole-brain irradiation with simultaneous integrated enhancement and demonstrates superior compliance and lower V44 in normal brain tissue compared to Helical TOMO or dynamic arc VMAT, the latter of which often exceeds safe dose thresholds for clinical use [95]. Small metastatic lesions (<3 cm) benefit from the exceptional accuracy of CK (nCI 1.168 ± 0.08), although its utility for larger targets is reduced due to impractical treatment times of > 200 min [44].

Pediatric tumors such as medulloblastoma and craniopharyngioma require special attention for neurocognitive preservation, where PBT has advantages by minimizing the output dose to developing brain structures. Pencil beam scanning technology of PBT (Fig. 4(a, b)) further enhances dose compliance for these cases, although long-term toxicity data remain limited (Fig. 4(c, d)) [30,88]. Spinal ependymomas (EPMs) represent another distinct category, where photon-IMRT remains the standard despite the growing interest in PBT, especially for pediatric cases where dose reduction to adjacent neural structures is critical (Fig. 4(e)) [89,101].

4.5. Future directions and clinical recommendations

The evolution of CNS tumor radiotherapy depends on overcoming current limitations while taking advantage of technological advances. The combination of evidence supports specific recommendations for each modality: VMAT appears as the preferred choice for resectable glioblastoma due to its balance of efficacy (CI 0.88–1.35) and reduced treatment time (294 MU vs. 572 MU for IMRT), while IMRT retains its value for cases requiring ultra-precise sparing of the OAR, such as optic nerve protection, where it achieves a Dmax of 11.34 Gy compared to 22.63 Gy with VMAT (Fig. 5(a, b)) [14,92]. For the pediatric population, PBT should be prioritized whenever possible, given its unique ability to limit hippocampal dose (Dmax 4.8 Gy vs. 52.5 Gy with photons) and reduce the risks of secondary malignancy, although its high cost (100 K–200 K per course) and limited availability make practical alternatives such as VMAT essential in resource-limited settings (Fig. 5(c, d)) [18,88,97].

Small metastatic lesions are ideally treated with CK when possible, while multifocal disease benefits from the integrated augmentation capabilities of P-VMAT [44,95]. Future research should focus on three critical areas: first, resolving the cost-access imbalance through the development of compact proton accelerators and shared resource models; second, validating the long-term outcomes of PBT pencil beam scans through multicenter registries [30,106]; and third, incorporating molecular biomarkers (e.g., MYCN amplification in spinal EPMs) to personalize dose administration (Fig. 6(a)) [107]. Clinical adoption

should be guided by practical considerations—for example, while a 15 % reduction in spinal Dmax of IGRT is dosimetrically desirable, its additional 20–30 min per segment may not be justified for rapidly progressing HGGs, emphasizing the need for context-specific protocols (Fig. 6(b, c)) [96].

Table 8 integrates these recommendations into an evidence-based framework, matching tumor scenarios with optimal methods, while explicitly grading the strength of the recommendation and acknowledging barriers to access. Bridging the gap between technology potential and real-world implementation will require concerted efforts in cost reduction, standardized reporting criteria, and prioritized comparative effectiveness trials, particularly for controversial areas such as PBT versus photon therapy in adult gliomas, where no difference in survival has been demonstrated despite theoretical benefits (Fig. 6(d)) [18,95].

5. Conclusion

This systematic review indicates that selecting the optimal radiation modality for CNS tumors necessitates careful consideration of tumor characteristics, patient factors, and available resources, with each technique providing distinct advantages in specific clinical scenarios. For pediatric cases, PBT offers superior outcomes by reducing hippocampal doses to 4.8 Gy (compared to 52.5 Gy with photons) while maintaining tumor control, with emerging AI-based adaptive planning systems enhancing delivery through automated optimization. CK offers excellent accuracy for small metastases (<3 cm) near vital structures (optic nerve Dmax 2.02 Gy), although its lengthy treatment sessions (220 min) may be alleviated by machine learning-based motion compensation algorithms. VMAT seems to be the most practical choice for multifocal metastases because of its high beam delivery efficiency (294 measurement units versus 572 measurement units in IMRT) and similar target coverage. However, IMRT still has value for complex cases that need ultra-precise sparing of the OAR, as shown by its lower optic nerve Dmax (11.34 Gy versus 22.63 Gy in VMAT) in *peri*-critical structures. The significant variability in dosimetry results underscores the need for standardized reporting and personalized planning, especially as AI-based decision support systems begin to integrate real-time imaging, tumor biology, and organizational resources to guide method selection. Future progress will depend on prospective trial testing techniques in molecularly defined subgroups, cost-effective analyses of advanced methods, and the implementation of federated learning networks to optimize rare tumor management. Together, these advances are transforming CNS radiotherapy from a one-size-fits-all approach to a dynamic optimization continuum that balances accuracy, practicality, and patient-specific outcomes.

Funding

This work was supported by the Tabriz University of Medical Sciences, Tabriz, Iran (Grant #73596) under the research ethics certificate IR.TBZMED.REC.1402.972.

Declaration of competing interest

The authors declare that they have no known competing financial interests or personal relationships that could have appeared to influence the work reported in this paper.

Acknowledgments

This study was supported by the Medical Radiation Science Research Team at Tabriz University of Medical Sciences, Tabriz, Iran.

Appendix A. Supplementary data

Supplementary data to this article can be found online at https://doi.org/10.1016/j.ejmp.2025.105682.

Data availability

All data generated or analyzed during this study are included in this published article and its Supplementary information files.

References

[1] Gregucci F, et al. Biological insights and radiation–immuno–oncology developments in primary and secondary brain tumors. Cancers 2024;16(11):2047.
[2] Ayyami Y, et al. Characterization and application of targeted MnO2/CS@ ALA-MTX nano-radiosensitizers for boosting X-ray radiotherapy of brain tumors. Colloids Surf A Physicochem Eng Asp 2024;692:133975.
[3] Kappel AD, et al. Endovascular applications for the management of high-grade gliomas in the modern era. Cancers 2024;16(8):1594.
[4] Ayyami Y, Ghorbani M, Dastgir M, Malekzadeh R, Mortezazadeh T. Chitosan-modified manganese oxide-conjugated methotrexate nanoparticles delivering 5-aminolevulinic acid as a dual-modal T1–T2* MRI contrast agent in U87MG cell detection. MAGMA 2024;37(5):909–24.
[5] Fuller CD, et al. Standard fractionation intensity modulated radiation therapy (IMRT) of primary and recurrent glioblastoma multiforme. Radiat Oncol 2007;2(1):26.
[6] Li W, et al. Advancing carbon ion therapy with dual-energy CT: enhanced elemental decomposition for precise range and secondary dose estimation. Phys Med 2025;133:104960.
[7] Major N, et al. The current state of radiotherapy for pediatric brain tumors: an overview of post-radiotherapy neurocognitive decline and outcomes. J Personalized Med 2022;12(7):1050.
[8] Vrtovec T, Močnik D, Strojan P, Pernuš F, Ibragimov B. Auto-segmentation of organs at risk for head and neck radiotherapy planning: from atlas-based to deep learning methods. Med Phys 2020;47(9):e929–50.
[9] Pourfarshid A, Mesbahi A, Mohammadzadeh M, Molazadeh M, Zeinali A. Dosimetric and radiobiological comparison of TomoTherapy and IMRT plans for prostate cancer. Radiat Phys Chem 2025;226:112356.
[10] Molazadeh M, Robatjazi M, Geraily G, Rezaeejam H, Zeinali A, Shirazi A. Three-dimensional IMRT QA of Monte Carlo and full scatter convolution algorithms based on 3D film dosimetry. Radiat Phys Chem 2021;186:109528.
[11] Asghari M, et al. Comparison of the effects of Govarcin herbal capsule and metoclopramide for alleviating gastrointestinal symptoms in patients with functional dyspepsia: a randomized double-blind clinical trial. Rev Recent Clin Trials 2024;19(2):143–9.
[12] Alterio D, et al. IMRT versus 2D/3D conformal RT in oropharyngeal cancer: a review of the literature and meta-analysis. Oral Dis 2021;27(7):1644–53.
[13] Souto C, et al. Beam data commissioning, validation and clinical implementation of SRS gyroscopic system. Phys Med 2025;133:104952.
[14] Sun M, Wang LL, Wang SQ, Lin X, Zhou W. Dosimetry comparison with helical tomotherapy, volumetric modulated arc therapy, and intensity-modulated radiotherapy for grade II gliomas: a single-institution case series. Open Life Sci 2023;18(1):20220550.
[15] Zhang HW, Hu B, Pang HW. Dosimetric comparison of helical tomotherapy and volumetric modulated arc therapy in hippocampal avoidance whole-brain radiotherapy. J Appl Clin Med Phys 2024;25(1):e14218.
[16] A. Zeinali, S. Ganjgahi, M. Mollazade, Evaluation of three-dimensional treatment planning system (TPS) performance in dose calculation of virtual wedged fields using film dosimetry, Iran J Med Phys, 15, Special Issue-12th. Iranian Congress of Medical Physics, 180–180, 2018.
[17] Michalski JM, et al. Children's oncology group phase III trial of reduced-dose and reduced-volume radiotherapy with chemotherapy for newly diagnosed average-risk medulloblastoma. J Clin Oncol 2021;39(24):2685–97.
[18] Seidel C, Heider S, Hau P, Glasow A, Dietzsch S, Kortmann R-D. Radiotherapy in medulloblastoma—evolution of treatment, current concepts and future perspectives. Cancers 2021;13(23):5945.
[19] Carter-Templeton H, et al., Completeness of systematic reviews in nursing literature based on PRISMA reporting guidelines, Adv Nurs Sci, 10.1097, 2025.
[20] Sterne JA et al., ROBINS-I: a tool for assessing risk of bias in non-randomised studies of interventions, BMJ, 355, 2016.
[21] Takaoka T, et al. Dosimetric comparison of helical tomotherapy and intensity-modulated proton therapy in hippocampus-and scalp-sparing whole brain radiotherapy. Technol Cancer Res Treat 2021;20:15330338211060170.
[22] Balasubramanian S, Shobana M, Anabalagan D, Thanasekar P, Joel S, Chaudhary P. Dosimetric and radiobiological comparison of IMRT, VMAT, and helical tomotherapy planning techniques in hippocampal sparing whole brain radiotherapy with simultaneous integrated boost for multiple brain metastases. Radiat Environ Biophys 2024;63(1):47–57.
[23] Kuru G, GÖKSEL E, Sakin R, Karaman S, Barburoglu M, Okutan M, Hippocampal sparing in stereotactic radiotherapy for multiple brain metastases: a comparison of intensity-modulated arc therapy, cyberknife, and helical radiotherapy, Turk Onkoloji Dergisi-Turkish J Oncol, 38, 2023.
[24] Liu P, et al. Comparison of dosimetric gains provided by intensity-modulated radiotherapy, volume-modulated arc therapy, and helical tomotherapy for high-grade glioma. Biomed Res Int 2020;2020(1):4258989.

[25] Song JH, et al. Dosimetric comparison of three different treatment modalities for total scalp irradiation: the conventional lateral photon–electron technique, helical tomotherapy, and volumetric-modulated arc therapy. J Radiat Res 2015; 56(4):717–26.
[26] Hsu S-M, Lai Y-C, Jeng C-C, Tseng C-Y. Dosimetric comparison of different treatment modalities for stereotactic radiotherapy. Radiat Oncol 2017;12:1–11.
[27] Greto D, et al. A dosimetric comparison between CyberKnife and tomotherapy treatment plans for single brain metastasis. Radiol Med 2017;122:392–7.
[28] Bishop AJ, et al. Proton beam therapy versus conformal photon radiation therapy for childhood craniopharyngioma: multi-institutional analysis of outcomes, cyst dynamics, and toxicity. Int J Radiat Oncol Biol Phys 2014;90(2):354–61.
[29] Dahshan BA, et al. Dose homogeneity analysis of adjuvant radiation treatment in surgically resected brain metastases: comparison of IORT, SRS, and IMRT indices. Brachytherapy 2021;20(2):426–32.
[30] Moteabbed M, Yock TI, Paganetti H. The risk of radiation-induced second cancers in the high to medium dose region: a comparison between passive and scanned proton therapy, IMRT and VMAT for pediatric patients with brain tumors. Phys Med Biol 2014;59(12):2883.
[31] Hermanto U, Frija EK, Lii MJ, Chang EL, Mahajan A, Woo SY. Intensity-modulated radiotherapy (IMRT) and conventional three-dimensional conformal radiotherapy for high-grade gliomas: does IMRT increase the integral dose to normal brain? Int J Radiat Oncol Biol Phys 2007;67(4):1135–44.
[32] Kim N, et al. Nomogram for radiation-induced lymphopenia in patients receiving intensity-modulated radiotherapy based-chemoradiation therapy for newly diagnosed glioblastoma: a multi-institutional study. Clin Transl Radiat Oncol 2024;47:100799.
[33] Skórska M, Piotrowski T, Kaźmierska J, Adamska K. A dosimetric comparison of IMRT versus helical tomotherapy for brain tumors. Phys Med 2014;30(4): 497–502.
[34] Sinaga AND, et al. Analisis variasi gantry terhadap distribusi dosis radiasi kanker otak dengan teknik intensity modulated radiation therapy (IMRT). Kappa J 2025; 9(1):110–5.
[35] Dunlop A, et al. Brain-sparing methods for IMRT of head and neck cancer. PLoS One 2015;10(3):e0120141.
[36] Tas B, Durmus I, Uzel O, Okumus A. Conformity index, gradient index, heterogeneity index, and size of metastasis correlations for LINAC-based stereotactic radiosurgery/radiation therapy. Int J Radiat Oncol Biol Phys 2017;99 (2):E727.
[37] Hridya V, Khanna D, Raj A, Padmanabhan S, Mohandass P. Dosimetric importance of the implementation of daily image guidance in radiotherapy practice. Asian Pac J Cancer Prev 2022;23(1):355.
[38] Kirkpatrick JP, et al. Defining the optimal planning target volume in image-guided stereotactic radiosurgery of brain metastases: results of a randomized trial. Int J Radiat Oncol Biol Phys 2015;91(1):100–8.
[39] Bell K, Licht N, Rübe C, Dzierma Y. Image guidance and positioning accuracy in clinical practice: influence of positioning errors and imaging dose on the real dose distribution for head and neck cancer treatment. Radiat Oncol 2018;13:1–13.
[40] El Shafie RA, et al. Single-isocenter volumetric modulated arc therapy vs. CyberKnife M6 for the stereotactic radiosurgery of multiple brain metastases. Front Oncol 2020;10:568.
[41] Duan Y, et al. Dosimetric comparison, treatment efficiency estimation, and biological evaluation of popular stereotactic radiosurgery options in treating single small brain metastasis. Front Oncol 2021;11:716152.
[42] Dong P, et al. Dosimetric characterization of hypofractionated Gamma Knife radiosurgery of large or complex brain tumors versus linear accelerator–based treatments. J Neurosurg 2016;125(Supplement_1):97–103.
[43] Guinement L, et al. Comparison between the HyperArc™ technique and the CyberKnife® technique for stereotactic treatment of brain metastases. Cancer/ Radiothérapie 2023;27(2):136–44.
[44] Shahban M, Rizwan MT, Nazia NS, Saeed UR, Humera M, Faheem M. Evaluation of intracranial stereotactic treatment plans: a comparison study of CyberKnife and TrueBeam systems. J Radiother Pract 2024;23:e12.
[45] Acker G, et al. Efficacy and safety of CyberKnife radiosurgery in elderly patients with brain metastases: a retrospective clinical evaluation. Radiat Oncol 2020;15: 1–10.
[46] Niu Y, et al. Comparative analysis of plan quality and delivery efficiency: ZAP-X vs. CyberKnife for brain metastases treatment. Available from Front Oncol 2024; 14:1333642. https://www.ncbi.nlm.nih.gov/pubmed/38939330.
[47] Miao Y, et al. Three-dimensional dose prediction based on deep convolutional neural networks for brain cancer in CyberKnife: accurate beam modelling of homogeneous tissue. BJR| Open 2024;6(1).
[48] Sio TT, Jang S, Lee SW, Curran B, Pyakuryal AP, Sternick ES. Comparing gamma knife and cyberknife in patients with brain metastases. J Appl Clin Med Phys 2014;15(1):14–26.
[49] Cho YH, et al. Experiences on two different stereotactic radiosurgery modalities of Gamma Knife and Cyberknife in treating brain metastases. Acta Neurochir 2015;157:2003–9.
[50] Berber T, Raturi V, Aksaray F, Hojo H, Fujisawa T, Ohyoshi H. Clinical outcome after CyberKnife® radiosurgery re-irradiation for recurrent brain metastases. Cancer/Radiothérapie 2021;25(5):457–62.
[51] Lautenschlaeger FS, et al. Comparison of carbon ion and photon reirradiation for recurrent glioblastoma. Strahlenther Onkol 2021:1–9.
[52] Harrabi SB, et al. Dosimetric advantages of proton therapy over conventional radiotherapy with photons in young patients and adults with low-grade glioma. Strahlenther Onkol 2016;192(11):759.
[53] Rydygier M, et al. Proton therapy adaptation of perisinusoidal and brain areas in the cyclotron centre bronowice in krakow: a dosimetric analysis. Cancers 2024;16 (18):3128.
[54] Chung CS, Yock TI, Nelson K, Xu Y, Keating NL, Tarbell NJ. Incidence of second malignancies among patients treated with proton versus photon radiation. Int J Radiat Oncol Biol Phys 2013;87(1):46–52.
[55] Ajithkumar T, et al. Proton therapy for craniopharyngioma—an early report from a single European centre. Clin Oncol 2018;30(5):307–16.
[56] Cao K, et al. Protontherapy of head and neck paragangliomas: a monocentric study. Cancer/Radiothérapie 2018;22(1):31–7.
[57] Vlachogiannis P, et al. Hypofractionated high-energy proton-beam irradiation is an alternative treatment for WHO grade I meningiomas. Acta Neurochir 2017; 159:2391–400.
[58] Murray FR, et al. Long-term clinical outcomes of pencil beam scanning proton therapy for benign and non-benign intracranial meningiomas. Int J Radiat Oncol Biol Phys 2017;99(5):1190–8.
[59] De Saint-Hubert M, et al. Complete patient exposure during paediatric brain cancer treatment for photon and proton therapy techniques including imaging procedures. Available from Front Oncol 2023;13:1222800. https://www.ncbi.nlm.nih.gov/pubmed/37795436.
[60] Liu P, et al. Comparison of dosimetric gains provided by intensity-modulated radiotherapy, volume-modulated arc therapy, and helical tomotherapy for high-grade glioma. Available from Biomed Res Int 2020;2020(1):4258989. https://www.ncbi.nlm.nih.gov/pubmed/32258121.
[61] Song JH, et al. Dosimetric comparison of three different treatment modalities for total scalp irradiation: the conventional lateral photon-electron technique, helical tomotherapy, and volumetric-modulated arc therapy. Available from J Radiat Res Jul 2015;56(4):717–26. https://www.ncbi.nlm.nih.gov/pubmed/24927727.
[62] Taufiqurrahman T, Rianto S, Setiawan AN. Comparative analysis of intensity modulation radiation therapy and volumetric modulation arc therapy in brain tumor cases to minimize radiation dose to organs at risk. IJSH 2023;2(10): 718–24.
[63] Hsu SM, Lai YC, Jeng CC, Tseng CY. Dosimetric comparison of different treatment modalities for stereotactic radiotherapy. Radiat Oncol 2017;12(1):155. Available from: https://www.ncbi.nlm.nih.gov/pubmed/28915893.
[64] Guinement L, et al. Comparison between the HyperArc technique and the CyberKnife(R) technique for stereotactic treatment of brain metastases. Available from Cancer Radiother Apr 2023;27(2):136–44. https://www.ncbi.nlm.nih.gov/pubmed/36797159.
[65] Dong P, et al. Dosimetric characterization of hypofractionated Gamma Knife radiosurgery of large or complex brain tumors versus linear accelerator-based treatments. Available from J Neurosurg Dec 2016;125(Suppl 1):97–103. https://www.ncbi.nlm.nih.gov/pubmed/27903198.
[66] Acker G, et al., Efficacy and safety of CyberKnife radiosurgery in elderly patients with brain metastases: a retrospective clinical evaluation, Radiat Oncol, vol. 15, no. 1, p. 225, Sep 29 2020. Available from: https://www.ncbi.nlm.nih.gov/pubmed/32993672.
[67] Miao et al Y, Three-dimensional dose prediction based on deep convolutional neural networks for brain cancer in CyberKnife: accurate beam modelling of homogeneous tissue, BJR Open, 6, 1, tzae023, Jan 2024. Available from: https://www.ncbi.nlm.nih.gov/pubmed/39220325.
[68] Sio TT, Jang S, Lee SW, Curran B, Pyakuryal AP, Sternick ES. Comparing gamma knife and cyberknife in patients with brain metastases. J Appl Clin Med Phys 2014;15(1):4095. Available from: https://www.ncbi.nlm.nih.gov/pubmed/24423830.
[69] Berber T, Raturi V, Aksaray F, Hojo H, Fujisawa T, Ohyoshi H. Clinical outcome after CyberKnife(R) radiosurgery re-irradiation for recurrent brain metastases. Available from Cancer Radiother Jul 2021;25(5):457–62. https://www.ncbi.nlm.nih.gov/pubmed/33752961.
[70] Cho YH, et al., Experiences on two different stereotactic radiosurgery modalities of Gamma Knife and Cyberknife in treating brain metastases," Acta Neurochir (Wien), 157, 11, 2003–9; discussion 2009, Nov 2015. Available from: https://www.ncbi.nlm.nih.gov/pubmed/26381540.
[71] Rydygier M, et al., Proton therapy adaptation of perisinusoidal and brain areas in the cyclotron centre bronowice in krakow: a dosimetric analysis, Cancers (Basel), 16, 18, 3128, Sep 11 2024. Available from: https://www.ncbi.nlm.nih.gov/pubmed/39335100.
[72] Chung CS, Yock TI, Nelson K, Xu Y, Keating NL, Tarbell NJ. Incidence of second malignancies among patients treated with proton versus photon radiation. Available from Int J Radiat Oncol Biol Phys 2013;87(1):46–52. https://www.ncbi.nlm.nih.gov/pubmed/23778197.
[73] Takaoka T, et al., Dosimetric comparison of helical tomotherapy and intensity-modulated proton therapy in hippocampus- and scalp-sparing whole brain radiotherapy, Technol Cancer Res Treat, 20, 15330338211060170, Jan–Dec 2021. Available from: https://www.ncbi.nlm.nih.gov/pubmed/34806489.
[74] Lautenschlaeger FS, et al. Comparison of carbon ion and photon reirradiation for recurrent glioblastoma. Available from Strahlenther Onkol May 2022;198(5): 427–35. https://www.ncbi.nlm.nih.gov/pubmed/34523017.
[75] Harrabi SB, et al. Dosimetric advantages of proton therapy over conventional radiotherapy with photons in young patients and adults with low-grade glioma. Available from Strahlenther Onkol Nov 2016;192(11):759–69. https://www.ncbi.nlm.nih.gov/pubmed/27363701.
[76] Bishop AJ, et al. Proton beam therapy versus conformal photon radiation therapy for childhood craniopharyngioma: multi-institutional analysis of outcomes, cyst dynamics, and toxicity. Available from Int J Radiat Oncol Biol Phys 2014;90(2): 354–61. https://www.ncbi.nlm.nih.gov/pubmed/25052561.

[77] Vlachogiannis P, et al. Hypofractionated high-energy proton-beam irradiation is an alternative treatment for WHO grade I meningiomas. Available from Acta Neurochir (Wien) Dec 2017;159(12):2391–400. https://www.ncbi.nlm.nih.gov/pubmed/29064038.
[78] Murray FR, et al. Long-term clinical outcomes of pencil beam scanning proton therapy for benign and non-benign intracranial meningiomas. Available from Int J Radiat Oncol Biol Phys 2017;99(5):1190–8. https://www.ncbi.nlm.nih.gov/pubmed/28939227.
[79] Cao KI, et al. Protontherapy of head and neck paragangliomas: a monocentric study. Available from Cancer Radiother Feb 2018;22(1):31–7. https://www.ncbi.nlm.nih.gov/pubmed/29269165.
[80] Ashour MG, Kamaleldin M, Mahmoud N, Barsoum EM, Abogabal AA, Dosimetric comparison of different radiotherapy techniques for scalp sparing whole brain radiotherapy.
[81] Alterio D, et al. IMRT versus 2D/3D conformal RT in oropharyngeal cancer: a review of the literature and meta-analysis. Available from Oral Dis Oct 2021;27 (7):1644–53. https://www.ncbi.nlm.nih.gov/pubmed/32810381.
[82] Gupta M, et al. Angle of concavity in planning target volume can be adopted as selection criteria for intensity-modulated radiation therapy or three-dimensional conformal radiotherapy technique in brain tumors. Available from J Cancer Res Ther Apr 2023;19(Supplement):S41–6. https://www.ncbi.nlm.nih.gov/pubmed/37147981.
[83] Washio H, Murata S, Ueda Y, Yamane Y, Konishi K. Accuracy of contour propagation from planning computed tomography to iterative cone-beam computed tomography using a deformable image registration algorithm for assisting head and neck radiotherapy. Phys Med 2025;133:104972.
[84] Ohhashi G, Miyazaki S, Ikeda H, Hori T, Postoperative long-term outcomes of patient with craniopharyngioma based on CyberKnife treatment, Cureus, 12, 3, 2020.
[85] Schwarz M, et al., IGRT versus non-IGRT for postoperative head-and-neck IMRT patients: dosimetric consequences arising from a PTV margin reduction, Radiat Oncol, 7, 133, Aug 8 2012. Available from: https://www.ncbi.nlm.nih.gov/pubmed/22873744.
[86] Xu Y, Xu Y, Men K, Xiao J, Dai J. Application of piecewise VMAT technique to whole-brain radiotherapy with simultaneous integrated boost for multiple metastases. Radiat Oncol 2022;17(1):86. Available from: https://www.ncbi.nlm.nih.gov/pubmed/35526019.
[87] Pollul G, et al. Pediatric craniospinal irradiation with a short partial-arc VMAT technique for medulloblastoma tumors in dosimetric comparison. Radiat Oncol 2020;15:1–10.
[88] Stripay JL, Merchant TE, Roussel MF, Tinkle CL. Preclinical models of craniospinal irradiation for medulloblastoma. Cancers 2020;12(1):133.
[89] Toescu SM, Aquilina K. Current and emerging methods of management of ependymoma. Curr Oncol Rep 2019;21:1–9.
[90] Kahn J, Loeffler JS, Niemierko A, Chiocca EA, Batchelor T, Chakravarti A. Long-term outcomes of patients with spinal cord gliomas treated by modern conformal radiation techniques. Int J Radiat Oncol Biol Phys 2011;81(1):232–8.
[91] Gregoire V, et al. Image guidance in radiation therapy for better cure of cancer. Available from Mol Oncol Jul 2020;14(7):1470–91. https://www.ncbi.nlm.nih.gov/pubmed/32536001.
[92] Navarria P, et al. Can advanced new radiation therapy technologies improve outcome of high grade glioma (HGG) patients? analysis of 3D-conformal radiotherapy (3DCRT) versus volumetric-modulated arc therapy (VMAT) in patients treated with surgery, concomitant and adjuvant chemo-radiotherapy. BMC Cancer 2016;16:1–10.
[93] Diaz MJ, et al. Current approaches to craniopharyngioma management. Front Biosci-Landmark 2022;27(12):328.
[94] Baliga S, et al. Decade-long disease, secondary malignancy, and brainstem injury outcomes in pediatric and young adult medulloblastoma patients treated with proton radiotherapy. Neuro Oncol 2022;24(6):1010–9.
[95] Xu Y, Xu Y, Men K, Xiao J, Dai J. Application of piecewise VMAT technique to whole-brain radiotherapy with simultaneous integrated boost for multiple metastases. Radiat Oncol 2022;17(1):86.
[96] Schwarz M, et al. IGRT versus non-IGRT for postoperative head-and-neck IMRT patients: dosimetric consequences arising from a PTV margin reduction. Radiat Oncol 2012;7:1–7.
[97] Jalali R, Sudarsan RT. Advances in radiation therapy in malignant brain tumors. Int J Neurooncol 2021;4(Suppl 1):S208–16.
[98] Dhawan S, Patil CG, Chen C, Venteicher AS, Early versus delayed postoperative radiotherapy for treatment of low-grade gliomas, Cochrane Database of Systematic Reviews, no. 1, 2020.
[99] Skorska M, Piotrowski T, Kazmierska J, Adamska K. A dosimetric comparison of IMRT versus helical tomotherapy for brain tumors. Available from Phys Med Jun 2014;30(4):497–502. https://www.ncbi.nlm.nih.gov/pubmed/24613513.
[100] Kearney M, Coffey M, Leong A. A review of image guided radiation therapy in head and neck cancer from 2009–2019–best practice recommendations for RTTs in the clinic. Techn Innov Patient Support Radiat Oncol 2020;14:43–50.
[101] Nunna RS, Khalid S, Ryoo JS, Mehta AI. Adult primary high-grade spinal glioma: a nationwide analysis of current trends in treatment and outcomes. J Neurooncol 2020;147:633–41.
[102] Pollul G, et al., Pediatric craniospinal irradiation with a short partial-arc VMAT technique for medulloblastoma tumors in dosimetric comparison, Radiat Oncol, 15, 1, 256, Nov 5 2020. Available from: https://www.ncbi.nlm.nih.gov/pubmed/33153495.
[103] Padovani L, Horan G, Ajithkumar T. Radiotherapy advances in paediatric medulloblastoma treatment. Available from Clin Oncol (R Coll Radiol) Mar 2019; 31(3):171–81. https://www.ncbi.nlm.nih.gov/pubmed/30655168.
[104] Navarria P, et al., Can advanced new radiation therapy technologies improve outcome of high grade glioma (HGG) patients? analysis of 3D-conformal radiotherapy (3DCRT) versus volumetric-modulated arc therapy (VMAT) in patients treated with surgery, concomitant and adjuvant chemo-radiotherapy, BMC Cancer, 16, 362, Jun 10 2016. Available from: https://www.ncbi.nlm.nih.gov/pubmed/27287048.
[105] Toescu SM, Aquilina K, Current and emerging methods of management of ependymoma, Curr Oncol Rep, 21, 9, 78, Jul 29 2019. Available from: https://www.ncbi.nlm.nih.gov/pubmed/31359299.
[106] Müller HL. Craniopharyngioma. Endocr Rev 2014;35(3):513–43.
[107] Louis DN, et al. The 2021 WHO classification of tumors of the central nervous system: a summary. Neuro Oncol 2021;23(8):1231–51.
[108] Bodensohn R, Haehl E, Belka C, Niyazi M. Fractionated radiotherapy for spinal tumors: a literature review regarding spinal glioma, ependymoma, and meningioma. Available from: Neurooncol Adv Oct 2024;6(Suppl):3. https://www.ncbi.nlm.nih.gov/pubmed/39430392.
[109] Mushtaq A, et al., Comprehensive analysis of craniopharyngioma: epidemiology, clinical characteristics, management strategies, and role of radiotherapy, Cancer Diagn Progn, 4, 4, 521–528, Jul–Aug 2024. Available from: https://www.ncbi.nlm.nih.gov/pubmed/38962549.
[110] Diaz MJ, et al., Current approaches to craniopharyngioma management, Front Biosci (Landmark Ed), 27, 12, 328, Dec 21 2022. Available from: https://www.ncbi.nlm.nih.gov/pubmed/36624954.
[111] Aggarwal A, Fersht N, Brada M. Radiotherapy for craniopharyngioma. Available from Pituitary Mar 2013;16(1):26–33. https://www.ncbi.nlm.nih.gov/pubmed/22948229.